

2m10

THE UNIVERSITY OF ALABAMA

COLLEGE OF ENGINEERING

BUREAU OF ENGINEERING RESEARCH

FINAL REPORT

on

Contract NAS8-20172

DESIGN OF FIR DIGITAL FILTERS FOR PULSE SHAPING AND
CHANNEL EQUALIZATION USING TIME-DOMAIN OPTIMIZATION

by

Ronald C. Houts
Project Director

and

Gregg L. Vaughn
Research Associate

Prepared for

National Aeronautics and Space Administration
George C. Marshall Space Flight Center
Marshall Space Flight Center, Alabama 35812

May 1974

BER Report No. 167-102



... UNIVERSITY, ALABAMA 35486

N74-29533

Unclass
45126

G3/08

CSCL 09B

92 p HC \$7.75

(NASA-CR-120340) DESIGN OF FIR DIGITAL
FILTERS FOR PULSE SHAPING AND CHANNEL
EQUALIZATION USING TIME-DOMAIN
OPTIMIZATION Final (Alabama Univ.,
University.)

DESIGN OF FIR DIGITAL FILTERS FOR
PULSE SHAPING AND CHANNEL EQUALIZATION
USING TIME-DOMAIN OPTIMIZATION

by

RONALD C. HOUTS
Project Director

and

GREGG L. VAUGHN
Research Associate

MAY, 1974

TECHNICAL REPORT NUMBER 167-102

Prepared for

National Aeronautics and Space Administration
Marshall Space Flight Center
Huntsville, Alabama

Under Contract Number

NAS8-20172

Communication Systems Group
Bureau of Engineering Research
The University of Alabama

ABSTRACT

Three algorithms are developed for designing finite impulse response (FIR) digital filters to be used for pulse shaping and channel equalization. The first is the Minimax algorithm which uses linear programming to design a frequency-sampling filter with a pulse shape that approximates the specification in a minimax sense. Symmetry restrictions are not required for the filter impulse response since the generated resonator coefficients are complex-valued. Also, the algorithm produces an efficient filter by selecting the resonators to include in the order of their decreasing contribution to the filter output. Design examples are included which accurately approximate a specified impulse response with a maximum error of 0.03 using only six resonators.

The second algorithm is an extension of the Minimax algorithm to design preset equalizers for channels with known impulse responses. Both transversal and frequency-sampling equalizer structures are designed to produce a minimax approximation of a specified channel output waveform. Examples of these designs are compared as to the accuracy of the approximation, the resultant intersymbol interference (ISI), and the required transmitted energy. While the transversal designs are slightly more accurate, the frequency-sampling designs using six resonators have smaller ISI and energy values.

The Energy-Minimization algorithm accomplishes equalizer design by using quadratic programming to minimize the transmitted energy while constraining the maximum error ϵ at any sampling point. Examples using this algorithm are compared with Minimax design examples for both transversal and frequency-sampling equalizers. Most of the Energy-Minimization designs required less transmitted energy and yield lower ISI than the corresponding Minimax designs. Also, the specification of ϵ provides a means of compromise between the energy required and the resultant ISI in the received waveform.

ACKNOWLEDGEMENT

The authors would like to express their appreciation to the Telemetry and Data Technology Branch of the Astrionics Laboratory, Marshall Space Flight Center, for the support of this research. The authors are grateful to Dr. D. W. Burlage for supplying data used for comparisons.

TABLE OF CONTENTS

	Page
ABSTRACT.	ii
ACKNOWLEDGEMENT	iv
LIST OF TABLES.	vii
LIST OF FIGURES	viii
CHAPTER 1 INTRODUCTION.	1
1.1 COMMUNICATION SYSTEM MODEL	1
1.2 BASEBAND COMMUNICATION PROBLEMS.	4
1.2.1 Intersymbol Interference.	4
1.2.2 Noise	5
1.2.3 Energy Constraints.	5
1.3 FINITE IMPULSE RESPONSE FILTERS.	6
1.3.1 Transversal Digital Filter.	6
1.3.2 Frequency-Sampling Digital Filter	8
1.4 SURVEY OF PERTINENT LITERATURE	12
1.5 OUTLINE OF STUDY	14
CHAPTER 2 TIME-DOMAIN DESIGN OF FIR DIGITAL FILTERS	16
2.1 FREQUENCY-SAMPLING FILTER DESIGN ALGORITHM.	17
2.2 DESIGN EXAMPLES.	19
2.2.1 Asymmetric Partial-Response Pulse	21
2.2.2 Raised-Cosine Pulse	22
2.2.3 Symmetric Partial-Response Pulse. . . .	25
2.2.4 Matched Filter for Ricker Wavelet	25
2.3 COMPARISON OF MINIMAX AND LINPO DESIGNS. . . .	25

	Page
CHAPTER 3 TIME-DOMAIN EQUALIZER DESIGN.	30
3.1 THE CHANNEL MODEL.	30
3.1.1 Mth-Order Lowpass Filter.	32
3.1.2 Telephone Channel	34
3.2 EQUALIZER DESIGN ALGORITHM	34
3.2.1 Transversal Equalizer	36
3.2.2 Frequency-Sampling Equalizer.	36
3.3 DESIGN EXAMPLES FOR LOWPASS CHANNELS	37
3.3.1 Transversal Designs	38
3.3.2 Frequency-Sampling Designs.	40
3.4 COMPARISON OF FREQUENCY-SAMPLING AND TRANSVERSAL DESIGNS FOR A TELEPHONE CHANNEL MODEL.	42
3.4.1 Frequency-Sampling Designs.	43
3.4.2 Transversal Designs	43
3.5 EXAMPLE OF EQUALIZED DATA TRANSMISSION	48
CHAPTER 4 ENERGY-MINIMIZATION EQUALIZER DESIGN.	50
4.1 ENERGY MINIMIZATION DESIGN	50
4.1.1 Transversal Equalizer	50
4.1.2 Frequency-Sampling Equalizer.	51
4.2 DESIGN EXAMPLES.	52
4.2.1 Transversal Designs	52
4.2.2 Frequency-Sampling Designs.	55
4.2.3 Distortion vs. Energy Trade-off	59
4.3 EXAMPLE OF EQUALIZED DATA TRANSMISSION	62
CHAPTER 5 SUMMARY AND RECOMMENDATIONS	64
APPENDIX A OPTIMIZATION AND FFT PROGRAMS	67
A.1 REVISED-SIMPLEX LINEAR PROGRAMMING	67
A.2 QUADRATIC PROGRAMMING USING THE WOLFE METHOD . .	69
A.3 FAST FOURIER TRANSFORM	70
APPENDIX B DESIGN PROGRAMS	72
B.1 MAIN DESIGN PROGRAMS	72
B.2 AUXILIARY SUBPROGRAMS.	79
LIST OF REFERENCES	80

LIST OF TABLES

Table		Page
2.1	RESONATOR COEFFICIENTS FOR DESIGN EXAMPLES	23
2.2	MINIMAX ERROR AND COMPUTATION TIME FOR DESIGN EXAMPLES.	24
2.3	COMPARISON OF LINPO AND MINIMAX PROCEDURE STEPS. . . .	27
2.4	COMPARISON OF LINPO AND MINIMAX FEATURES	28
2.5	COMPARISON OF LINPO AND MINIMAX SOLUTIONS.	29
3.1	COMPARISON OF DESIGN RESULTS FOR LOWPASS CHANNELS. . .	39
3.2	FREQUENCY-SAMPLING EQUALIZER DESIGNS FOR RAISED-COSINE PULSES (N = 60).	44
3.3	FREQUENCY-SAMPLING EQUALIZER DESIGNS FOR PARTIAL RESPONSE PULSES ($B = 6$, $T_b = 0.05$)	45
3.4	FREQUENCY-SAMPLING EQUALIZER DESIGN RESULTS.	46
3.5	TRANSVERSAL EQUALIZER DESIGNS.	47
4.1	CONSTRAINT POINTS FOR ENERGY-MINIMIZATION DESIGNS. . .	53
4.2	COMPARISON OF TRANSVERSAL EQUALIZER DESIGN EXAMPLES. .	54
4.3	COMPARISON OF FREQUENCY-SAMPLING EQUALIZER DESIGN EXAMPLES FOR TELEPHONE CHANNEL.	57
4.4	COMPARISON OF FREQUENCY-SAMPLING EQUALIZER DESIGN EXAMPLES FOR BPF CHANNEL.	58
B.1	INPUT DATA FOR DESIGN PROGRAMS	78

LIST OF FIGURES

Figure	Page
1-1 Communication System Model	2
1-2 Transversal Filter	7
1-3 Frequency-Sampling Filter.	9
1-4 Digital Resonators	11
2-1 Frequency-Sampling Filter Design Examples.	20
3-1 Impulse Response and Amplitude Characteristic for Mth-Order Lowpass Channel Model.	33
3-2 Telephone Channel Model.	35
3-3 Comparing Receiver Waveforms for Linpo and Minimax Transversal Equalizers with 6th-Order Channel.	41
3-4 Effect of Minimax Designed Equalizer on 15 Bit PN Sequence Transmitted Over Telephone Channel.	49
4-1 Bandpass Filter Channel Model.	56
4-2 Time-Domain Responses for Energy-Minimization Algorithm. . .	60
4-3 Compromise Between ISI and Transmitted Energy by the Selection of ϵ	61
4-4 Effect of Energy-Minimization Designed Equalizer on 15 Bit PN Sequence Transmitted Over Telephone Channel	63
B-1 Minimax Pulse Shaping Digital Filter Design Program.	73
B-2 PSRCT, Minimax Transversal Equalizer Design Program.	74
B-3 PSRCF, Minimax Frequency-Sampling Equalizer Design Program .	75
B-4 EMRCT, Energy-Minimization Transversal Equalizer Design Program	76
B-5 EMRCF, Energy-Minimization Frequency-Sampling Equalizer Design Program	77

CHAPTER 1

INTRODUCTION

More reliable communication can be achieved if the problems associated with the communication path, or channel, are overcome. This study considers a baseband communication system using pulse amplitude modulation (PAM). The problems considered are limited channel bandwidth, intersymbol interference (ISI), noise, and transmitted-signal energy limitations. Two types of finite impulse response (FIR) digital filters are examined for use as equalizers and/or pulse shaping filters in an effort to solve the problems. Design procedures for these filters and design examples showing their application to ideally bandlimited or more realistic channels are included.

1.1 COMMUNICATION SYSTEM MODEL

The communication system model used in this study is shown in Fig. 1-1. The data source generates a sequence of symbols $\{a(k)\}$ at a rate of $1/T_b$ per second (s). The possible values that $a(k)$ may assume are restricted, i.e., $a(k)$ is either a continuous variable limited to some range or a discrete variable which assumes one of a finite set of values. In the case of binary signaling only the two values ± 1 are allowed.

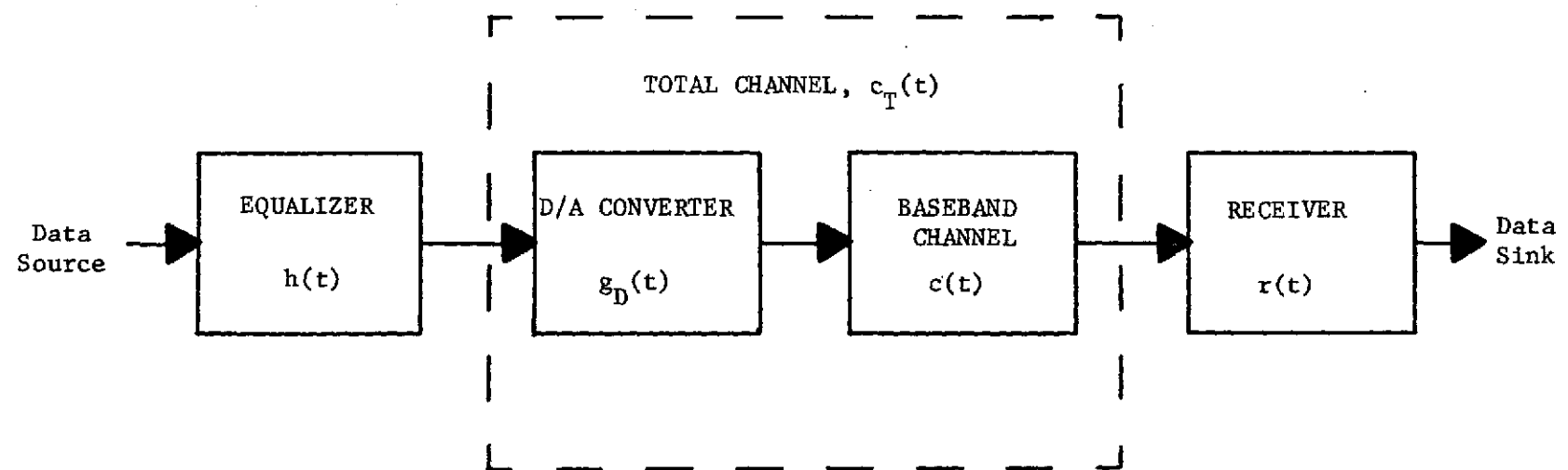


Fig. 1-1. Communication System Model.

The equalizer is a digital filter used to compensate for the distortion introduced by the channel. The equalizer output is given by

$$\begin{aligned}
 s(t) &= \sum_k a(k) h(t - kT_b) \\
 &= \sum_k a(k) \sum_n h(n) \delta(t - kT_b - nT),
 \end{aligned} \tag{1.1}$$

where $h(t)$ is the impulse response of the digital filter, T is time between output samples, and T_b is the time between input symbols. The discrete-time output of the equalizer, or transmitter, is converted to continuous time by the digital-to-analog (D/A) converter which has a zero-order hold impulse response, $g_D(t) = u(t) - u(t - T)$, where T is the sampling interval. In passing through the baseband channel $c(t)$, the continuous-signal waveform is altered due to the channel's amplitude and phase characteristic plus additive noise. The baseband channel has a lowpass frequency characteristic $C(f)$, but it generally lacks dc response. For convenience the D/A converter is grouped with the baseband channel to form the total channel with impulse response $c_T(t)$.

At the receiver an attempt is made to reconstruct the transmitted symbol sequence. The simplest type of receiver is a single-sample detector in which the received waveform is sampled once every T_b s. The receiver then chooses the symbol whose value is closest to the sample value.

1.2 BASEBAND COMMUNICATION PROBLEMS

Three basic problems hinder the receiver from producing an accurate replica of the transmitted symbol sequence: ISI, noise, and maximum energy limitations of the transmitter and channel.

1.2.1 Intersymbol Interference

The bandwidth limitations and nonlinear phase characteristics of realistic channels cause a pulse to be dispersed in time. One pulse may be spread in time to the extent that it interferes with the detection of several adjacent pulses. Even in the absence of noise, receiver errors may exist because of ISI.

A received pulse $y(t)$ is described mathematically by the convolution of the transmitted pulse $h(n) \delta(t - nT)$ and the impulse response of the total channel $c_T(t)$. The composite received waveform can be written as

$$y_c(t) = \sum_k y(t - kT_b). \quad (1.2)$$

If single-sample detection is used, the maximum amount of distortion caused by one pulse is called the total peak ISI distortion D , i.e.,

$$D \triangleq \sum_{\substack{k=-\infty \\ k \neq 0}}^{\infty} |y(kT_b)|. \quad (1.3)$$

Complete elimination of ISI is achieved when each received pulse has zero magnitude at the sampling times of all other pulses. Nyquist [1] determined a class of pulses which exhibit this property. For each of these pulses the composite frequency characteristic is flat

over a bandwidth of $1/(2T_b)$ Hz. That is, the sum of the frequency response of the pulse and all aliasing caused by sampling every T_b s is a constant over the bandwidth $1/(2T_b)$ Hz. Pulses of the Nyquist class are not physically realizable but can be closely approximated.

1.2.2 Noise

Noise in the channel is modeled by a term $n(t)$ added to the received waveform (1.2), where $n(t)$ is assumed to be a sample function of a stationary, white Gaussian random process. For channels with low signal-to-noise ratios (SNR), optimum reception in the presence of noise is more important than overcoming the problem of ISI. It has been shown [2] that a receiver filter matched to the received pulse gives optimum performance in the presence of such noise. The matched filter has an impulse response $r(t) = y(T_b - t)$, and the filter output at time $t = T_b$ is the optimum measure in an SNR sense of the transmitted symbol value. The received pulse is assumed to have negligible amplitude outside the interval $0 < t < T_b$.

1.2.3 Energy Constraints

For a given channel the optimum signal energy-density distribution strategy [3] is to shape the spectrum of the transmitted pulse $S(f)$ so it will not be attenuated significantly by the channel since the received signal energy-density spectrum is proportional to $|S(f)|^2 |C(f)|^2$. However, for zero ISI the overall frequency characteristic of the transmitter, channel, and receiver must satisfy the Nyquist criterion over a bandwidth $W \leq 1/2T_b$ Hz and zero elsewhere [4]. This implies that signal energy often must be forced through the channel, in the bandwidth W , where its attenuation is the greatest in order to provide the overall Nyquist characteristic. A

large amount of energy may be required of the transmitter, very little of which is available at the receiver. A transmitter operating at a given power level P with a fixed signaling interval T_b establishes an upper limit PT_b on the amount of energy in each pulse. Furthermore, many channels have a practical limit on the power that can be applied to the channel. A compromise must be reached between the conflicting requirements for large energy required for ISI-free transmission and the fixed energy available for a transmitter operating with specified power and signal rates.

1.3 FINITE IMPULSE RESPONSE FILTERS

Transversal and frequency-sampling digital filters are two realizations of a FIR filter, whose impulse response $\{h(n)\}$ is non-zero only for N consecutive sample points.

1.3.1 Transversal Digital Filter

A transversal digital filter is a digital version of a tapped delay line. As shown in Fig. 1-2, the transversal filter consists of an N -stage shift register and N digital multipliers commonly referred to as tap gains. The filter is designed by specifying the number of shift-register stages N and the set of tap gains $\{h(n)\}$. The difference equation relating the filter input and output can be written by inspection.

$$y(n) = \sum_{k=0}^{N-1} h(k) x(n - k). \quad (1.4)$$

Taking the z -transform of $h(n)$ yields the corresponding transfer

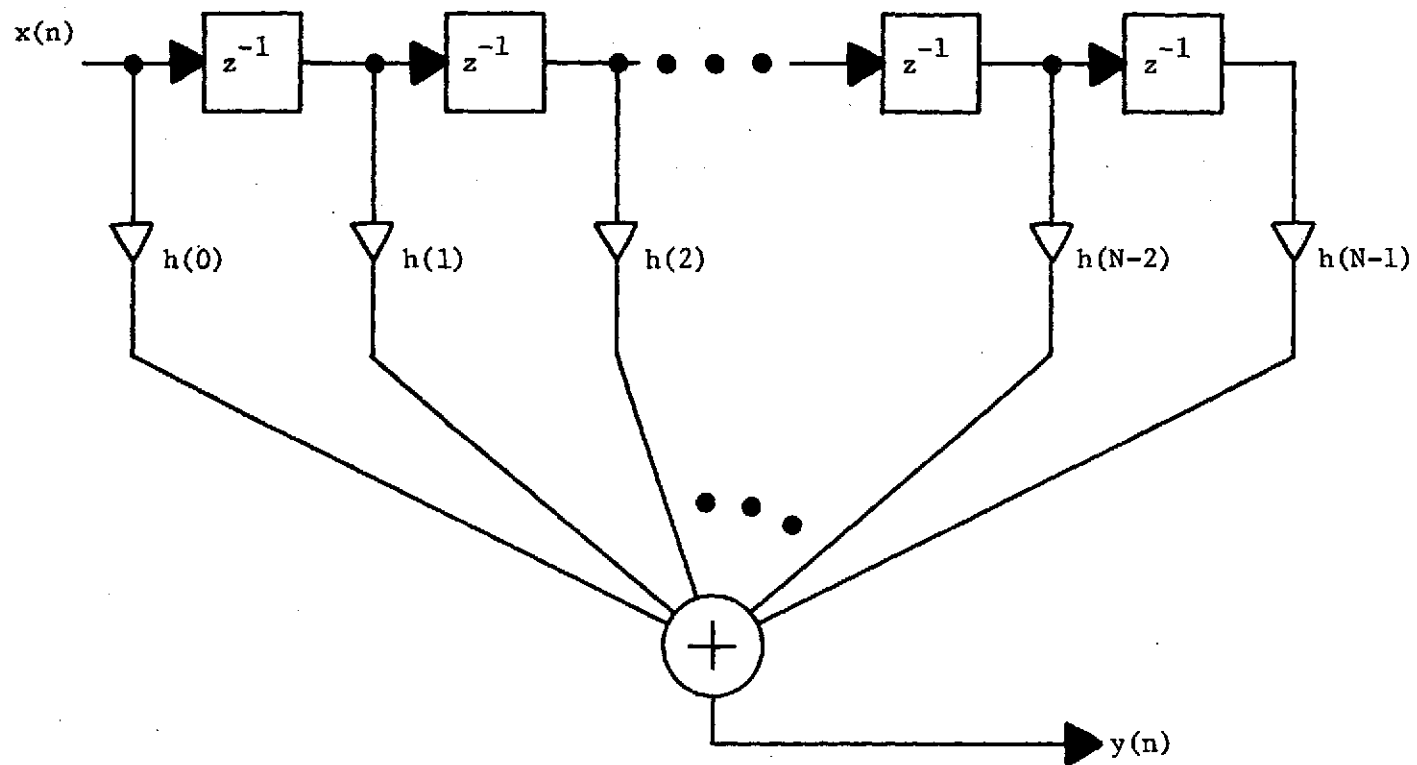


Fig. 1-2. Transversal Filter.

function, i.e.,

$$H(z) = \sum_{n=0}^{N-1} h(n) z^{-n}. \quad (1.5)$$

Since (1.5) contains no poles, the transversal realization is inherently stable.

1.3.2 Frequency-Sampling Digital Filter

A frequency-sampling filter consists of a comb filter in cascade with a parallel bank of $1 + N/2$ or fewer first- and second-order digital resonators, as shown in Fig. 1-3. Associated with each resonator is a filter coefficient $H(k)$, called a frequency sample, which can be obtained by replacing z^{-n} by $\exp(-j2\pi kn/N)$ in (1.5). The name "frequency sampling" comes from the original design procedure [5] in which it was desired to approximate a continuous frequency response by a set of samples $\{H(k)\}$ taken every $1/NT$ Hz, from dc to $1/2T$, the half-sampling frequency. Taking the inverse discrete Fourier transform (IDFT) of the frequency samples yields the filter impulse response.

$$h(n) = \frac{1}{N} \sum_{k=0}^{N-1} H(k) \exp(j2\pi kn/N). \quad (1.6)$$

The continuous frequency response of the filter has the desired values at the frequency samples. Substituting (1.6) into (1.5) yields

$$H(z) = \sum_{n=0}^{N-1} \left[\frac{1}{N} \sum_{k=0}^{N-1} H(k) \exp(j2\pi kn/N) \right] z^{-n}, \quad (1.7)$$

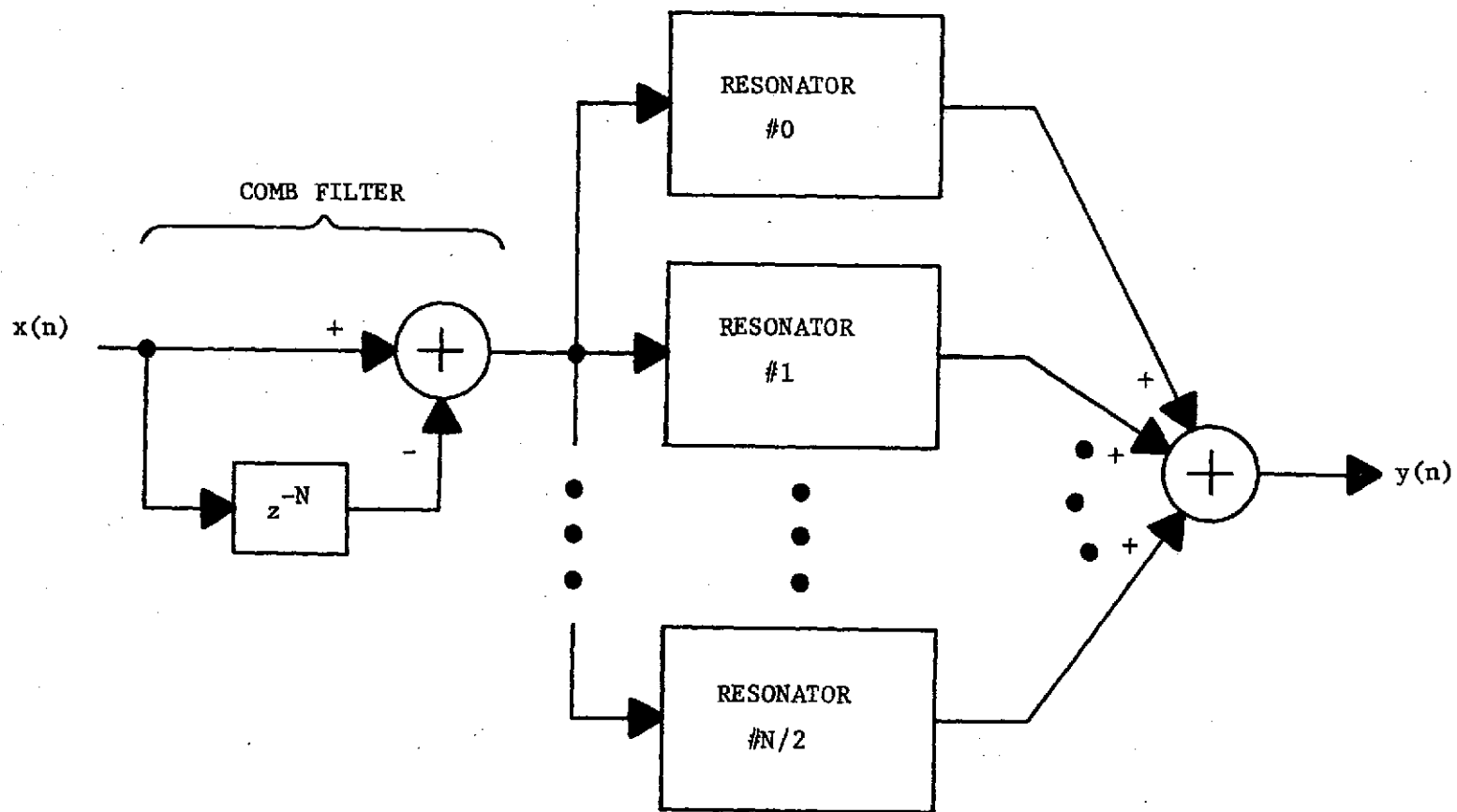


Fig. 1-3. Frequency-Sampling Filter.

which by exchanging the order of summation gives

$$H(z) = \frac{1 - z^{-N}}{N} \sum_{k=0}^{N-1} \frac{H(k)}{1 - \exp(j2\pi k/N)z^{-1}}. \quad (1.8)$$

The frequency samples are assumed to be complex valued, i.e., $H(k) = X(k) + jY(k)$; however, the impulse response $\{h(n)\}$ is assumed to be real valued, which implies that

$$\begin{aligned} X(k) &= X(N - k), \\ Y(k) &= -Y(N - k), \\ Y(0) &= 0. \end{aligned} \quad (1.9)$$

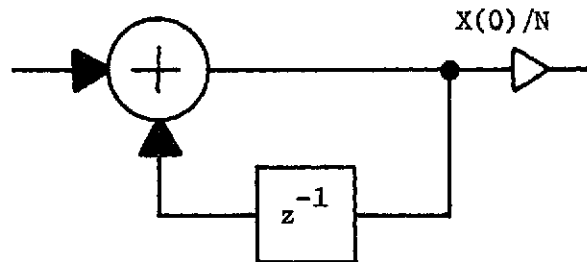
Thus (1.8) can be simplified by combining exponentials. For N even

$$H(z) = \frac{1 - z^{-N}}{N} \left[\frac{X(0)}{1 - z^{-1}} + \frac{X(N/2)}{1 + z^{-1}} + \sum_{k=1}^{N/2-1} \frac{2X(k) - 2[X(k) \cos(2\pi k/N) + Y(k) \sin(2\pi k/N)]z^{-1}}{1 - 2z^{-1} \cos(2\pi k/N) + z^{-2}} \right]. \quad (1.10)$$

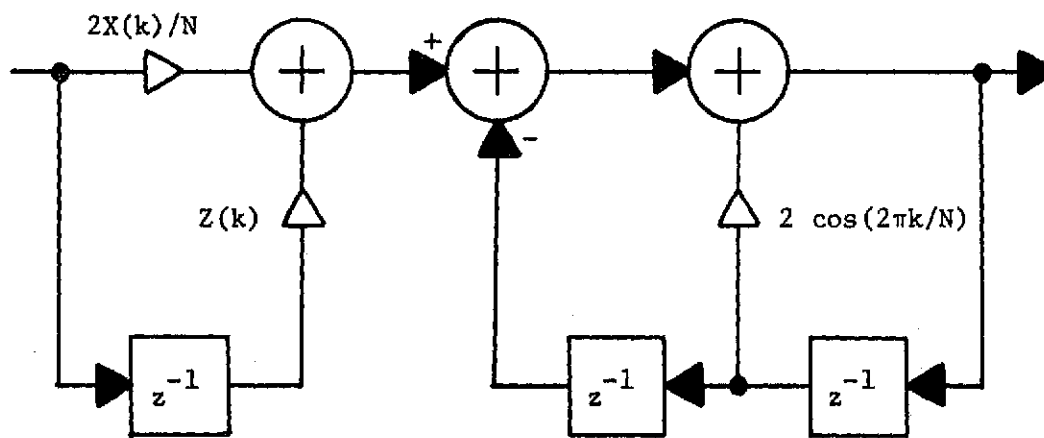
The forms of the first- and second-order resonators are shown in Fig. 1-4. In a similar way (1.6) can be written in the form

$$\begin{aligned} h(n) &= \frac{X(0) + (-1)^n X(N/2)}{N} + \\ &\quad \frac{2}{N} \sum_{k=1}^{N/2-1} [X(k) \cos(2\pi kn/N) - Y(k) \sin(2\pi kn/N)]. \end{aligned} \quad (1.11)$$

In a frequency-sampling filter the comb filter contributes zeros which are uniformly spaced around the unit circle in the z plane. The desired frequency characteristic is formed by using



(a) First-Order Resonator



$$Z(k) \triangleq -2[X(k) \cos(2\pi k/N) + Y(k) \sin(2\pi k/N)]/N$$

(b) Second-Order Resonator

Fig. 1-4. Digital Resonators.

resonator poles to cancel selected zeros depending on whether the filter is lowpass, bandpass, etc. Because the poles lie on the unit circle, frequency-sampling filters can be unstable; however, the stability can be assured without measurably altering the filter characteristics by moving the poles and zeros slightly inside the unit circle [5].

1.4 SURVEY OF PERTINENT LITERATURE

A summary of the historical developments in baseband communication systems is found in the report by Houts and Burlage [6]. However, some of the pertinent articles in the areas of intersymbol interference, signal energy considerations, and digital filter design techniques are summarized in this section. Hancock [7] studied the problem of choosing optimum signaling waveforms for digital communication over a known channel. Under the constraint of no ISI many possible waveforms exist. Hancock's method was to choose the one with the largest received energy, since this was optimum for a matched filter receiver. He also investigated the trade-off between elimination of ISI and minimization of transmitted energy. Schweppe [8] proposed a general method for choosing signaling waveforms for ideal bandlimited channels to minimize the probability of error. The energy in the waveforms was not constrained although the waveforms were assumed to not overlap in time. Snyder and Blaine [9] studied binary signaling over a known channel with additive white Gaussian noise and presented a method for joint optimization of the transmitted waveform

and the receiver with constraints on the energy, peak amplitude, and bandwidth of the transmitted pulse. In their work the waveforms were not allowed to overlap in time.

Recent research in FIR digital filter design has centered around the use of linear and nonlinear programming techniques to provide designs which are optimal in some sense. Rabiner has published several papers[10-14] on the subject of FIR digital filter design. His methods use frequency-domain objective functions which are minimized subject to constraints in the frequency and time domains. The filters are assumed to have linear phase characteristics. Cavin, Ray, and Rhyne [15] have used linear programming to design a convolutional digital filter to be used as a receiver for Ricker wavelets. The filter was designed to produce an output spike whenever a Ricker wavelet was detected. Helms [16] has summarized several optimization techniques using both linear and nonlinear programming to design digital filters from frequency-domain specifications. Burlage and Houts [17] have described a method for designing transversal and frequency-sampling digital filters from time-domain specifications. Linear programming was used with the objective function and constraints written about critical points in the desired waveform. Digital equalizers were designed [18] by writing the objective function and constraints about points in the channel output waveform. However, their method relied on the user's ability to choose the critical points, and it did not guarantee a solution. The frequency-sampling filters were assumed to have a linear phase characteristic, and, as a result, the transversal realization was considered better for use as an

equalizer. It was observed that the energy in the transmitted pulse increased drastically as constraints were added to the received waveform between established zero crossings because this required energy to be transmitted through the channel at frequencies where the attenuation was severe. The transmitted energy required was dependent upon the ratio of sampling interval to pulse interval T/T_b , with a minimum energy occurring in the vicinity of $T/T_b = 0.4$ for the particular channel under study.

1.5 OUTLINE OF STUDY

This chapter has outlined the basic problems in baseband communication systems, the previous efforts to solve these problems, and the two types of FIR digital filters which will be employed in the equalizer. The optimum design of FIR filters for pulse shaping is the topic of Chapter 2. The applications considered are matched-filter detection and equalization of an unknown band-limited channel. Since the channel characteristic is unknown, it is assumed to be ideal lowpass. The pulse-shaping design algorithm is expanded in Chapter 3 to include communication systems in which the channel impulse-response is known. The problem of designing a filter to jointly combat the ISI and energy minimization problems is discussed in Chapter 4. The final chapter contains conclusions and recommendations for further study. Throughout this study it is assumed that the channel has a high SNR, i.e., the primary source of errors is ISI. Brief explanations of the theory and purposes of the computer programs used in the filter design are found in the appendices. The two optimization routines, revised-simplex linear

programming and quadratic programming by the Wolfe algorithm, and the fast Fourier transform (FFT) are discussed in App. A. The operation of the various main programs used in the aforementioned designs and the purposes of the various utility subprograms called by the main design programs are described in App. B.

CHAPTER 2

TIME-DOMAIN DESIGN OF FIR DIGITAL FILTERS

Digital filters designed to have specified impulse responses can be used in baseband communication systems for pulse shaping and matched filters. For an ideal bandlimited channel ISI is eliminated when the signaling pulse shapes are of the Nyquist [4] class. Optimum noise performance is obtained using receiver filters matched to the received pulses.

Often the desired continuous-time impulse response $d(t)$ is essentially zero outside some time interval NT s. Consequently, the first step in the time-domain design is to restrict the desired response to NT s so that it can be approximated by a FIR digital filter. A desired discrete-time response $\{d(n)\}$ is obtained from N uniformly spaced samples of $d(t)$,

$$d(n) \triangleq d(nT - \tau) \quad n = 0, 1, \dots, N-1, \quad (2.1)$$

where τ is a time delay included to shift the desired response out of negative time. The designer must choose the number of samples N and the sampling interval T to represent the characteristics of the desired impulse response.

At this point the design of the transversal filter realization is complete since the N impulse-response samples are the filter

tap gains. However, it may be possible to approximate $\{d(n)\}$ accurately using a frequency-sampling realization with fewer than N multiplications, depending on the number of resonators R in the design. The number of multiplications constrains either the operation speed or the equipment complexity of the filter. If the multiplications are performed in sequence on one hardware multiplier, the minimum sample time T is determined by the number of multiplications and the speed of the multiplier. Alternatively, if the multiplications are performed in parallel on N individual hardware multipliers, the equipment complexity increases accordingly.

2.1 FREQUENCY-SAMPLING FILTER DESIGN ALGORITHM

The Minimax algorithm produces a filter whose impulse response $\{h(n)\}$ is a minimax approximation of the desired response $\{d(n)\}$. The resonator coefficients are allowed to take on complex values and the resonators are added to the design in the order of their decreasing contribution to the solution. The number of resonators R included in the design is increased until the approximation error is acceptable.

The design algorithm chooses the filter coefficients $\{H(k)\}$ to minimize the maximum absolute difference $|d(n)-h(n)|$ over all n , i.e.,

$$\text{Min} \left[\text{Max}_{0 \leq n \leq N-1} |d(n) - h(n)| \right]. \quad (2.2)$$

It was shown in (1.11), which is repeated as (2.3), that $h(n)$ can be

expressed in terms of the unknown frequency samples $\{H(k) \triangleq X(k) + jY(k)\}$.

$$h(n) = \frac{X(0) + (-1)^n X(N/2)}{N} + \frac{2}{N} \sum_{k=1}^{N/2-1} [X(k) \cos(2\pi kn/N) - Y(k) \sin(2\pi kn/N)]. \quad (2.3)$$

Since R resonators are to be included in the filter design, only R of the $\{H(k)\}$ are allowed to have non-zero values, i.e., $H(k) = 0$ for all k which are not elements of the set $\{S(1), S(2), \dots, S(R)\}$. Because (2.3) is a linear combination of the real and imaginary parts of the non-zero filter coefficients, the minimization of (2.2) may be expressed as the following linear programming (LP) problem:

$$\begin{aligned} &\text{Minimize: } \epsilon \\ &\text{Subject to: } h(n) + \epsilon \geq d(n) \\ &\qquad\qquad\qquad h(n) - \epsilon \leq d(n) \end{aligned} \quad \begin{aligned} & n = 0, 1, \dots, N-1. \end{aligned} \quad (2.4)$$

The optimal value of ϵ is the maximum of the errors $e(n) \triangleq h(n) - d(n)$ over the N sample points, i.e.,

$$\epsilon = \max_{0 \leq n \leq N-1} |e(n)|. \quad (2.5)$$

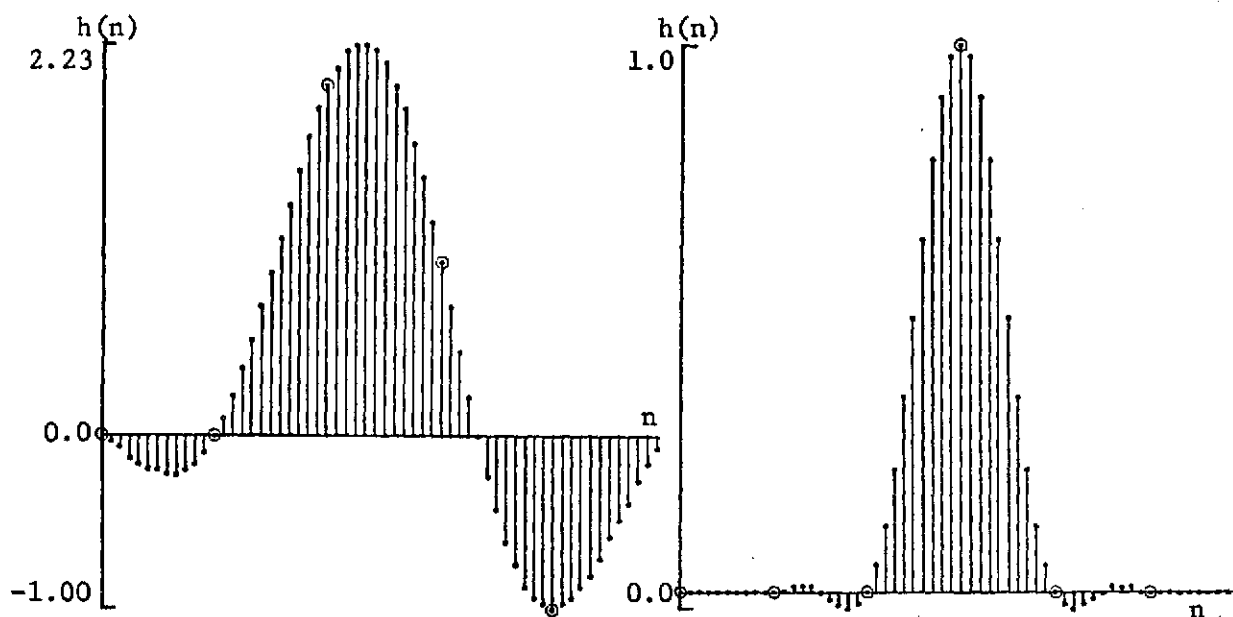
Equation (2.4) is solved using the revised-simplex linear programming algorithm discussed in App. A.

The algorithm chooses which resonators to include in $\{S(i)\}$ using an iterative procedure. Starting with $R = 0$, resonators are added to the design one at a time in the order of decreasing

contribution to the solution until either R equals some specified maximum allowable value or ϵ is less than some acceptable value. During each iteration resonators are considered candidates to be added to the design in the order of the decreasing magnitudes of their corresponding coefficients in $\{E(k)\}$, the DFT of $\{e(n)\}$, which is obtained using FFT techniques described in App. A. A candidate is temporarily added to the design and (2.4) is solved. If the value of ϵ is reduced, the candidate is replaced by the next candidate and (2.4) is solved again, etc. However, once the value of ϵ is increased, the previous candidate is permanently added to the solution; and the next iteration begins with one less candidate available for inclusion as the next resonator.

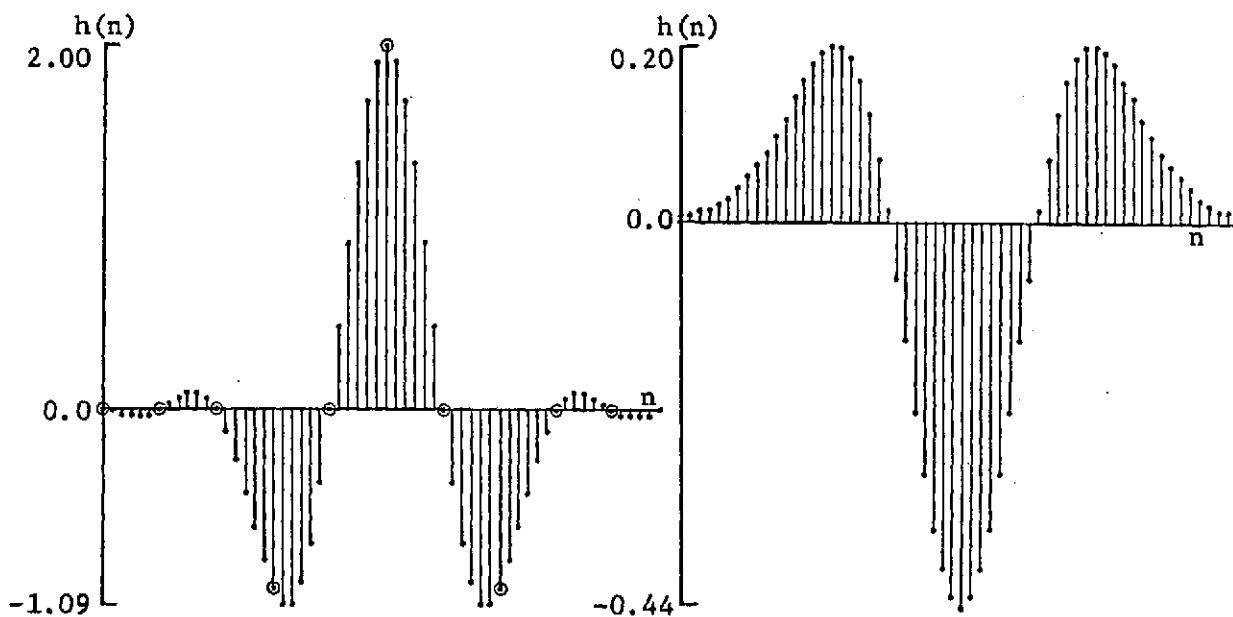
2.2 DESIGN EXAMPLES

Four examples are presented to illustrate the applicability of the Minimax design algorithm. In each example a desired continuous time pulse is given with an interval of time NT in which the approximation is to be made. Outside of this interval the pulse is very close to zero and is so approximated. Inside the time interval the pulse is sampled at N equally spaced points. For all four examples a set of samples ($N = 60$) was considered sufficient to accurately describe the pulse $\{d(n)\}$, which was supplied as input to the Minimax algorithm. It was further assumed that practical considerations [11] limited the maximum number of resonators to six, i.e., $R \leq 6$. The filter output waveforms for the four examples are illustrated in Fig. 2-1. The first three examples are useful as



(a) Asymmetric Partial-Response Pulse ($B = 12$)

(b) Raised-Cosine Pulse ($B = 10$)



(c) Symmetric Partial-Response Pulse ($B = 6$)

(d) Ricker Wavelet

Fig. 2-1. Frequency-Sampling Filter Design Examples.

PAM signaling pulses. The pulse-shaping filter would be used in a baseband communication system with a channel modeled as ideal with bandwidth sufficient to pass the spectral components of the transmitted pulses. A weighted unit-pulse $a(n)\delta(n)$ is applied to the filter input every T_b s or every B th-sample, i.e., $T_b \triangleq BT$, all $B-1$ intermediate inputs being zero.

2.2.1 Asymmetric Partial-Response Pulse

The first example is an asymmetric partial-response pulse. Using this type pulse permits signaling at a rate of twice the channel bandwidth by allowing a controlled amount of ISI. In the conventional baseband signaling scheme, where ISI is forced to zero by requiring the received pulse to have zeros at all sampling times about the peak, the signaling rate can not exceed the channel bandwidth. The expression for the desired impulse response samples for $B = 12$ is

$$d(n) = 2 \operatorname{sinc}(C+0.5) + \operatorname{sinc}(C-0.5) - \operatorname{sinc}(C-1.5), \quad (2.6)$$

where

$$C \triangleq (n - N/2)/B, \quad (2.7a)$$

and

$$\operatorname{sinc}(x) \triangleq \sin(\pi x)/(\pi x). \quad (2.7b)$$

These two definitions are also employed in the other three design examples. The filter impulse response for the design with the six resonators selected in the order $\{1,2,0,3,4,6\}$ is shown in Fig.

2-1(a). These samples differ from the desired samples by at most 0.0279. The design results for one through six resonators are compared in Tables 2.1 and 2.2 with similar comparisons for the other three examples. Notice that in this first example the filter coefficients given in Table 2.1 included both real and imaginary parts. At each iteration one new resonator is added, and the coefficients of all the resonators currently in the design are recalculated. The resonator added each time is the one which will produce the smallest maximum error ϵ , as listed in Table 2.2. Because the frequency samples are complex valued, the time required for a given iteration is considerably longer than the other examples.

2.2.2 Raised-Cosine Pulse

The second example is the raised-cosine pulse which has zero crossings every T_b s measured with respect to the pulse peak. The filter impulse response for $R = 6$ is shown in Fig. 2-1(b), and the samples are given by (2.8) with $\alpha = 1$. The value of α may range from 0 to 1 and is the fraction by which the pulse bandwidth exceeds the Nyquist bandwidth.

$$d(n) = \text{sinc}(C) \frac{\cos(\alpha\pi C)}{(1 - 4\alpha^2 C^2)}, \quad (2.8)$$

where C is defined by (2.7a) with $B = 10$. Since the desired impulse response is symmetric about its midpoint, it follows that the set of frequency samples $\{H(k)\}$ is real valued. Consequently, the time required to perform an iteration is considerably less than the general case as can be seen from Table 2.2.

TABLE 2.1

RESONATOR COEFFICIENTS FOR DESIGN EXAMPLES

R	ASYMMETRIC PARTIAL RESPONSE			RAISED COSINE		SYMMETRIC PARTIAL RESPONSE		RICKER WAVELET	
	k	X(k)	Y(k)	k	X(k)	k	X(k)	k	X(k)
1	1	-31.831	-23.585	2	14.778	3	-29.527	2	-6.495
2	1	-32.439	-19.142	2	5.892	3	-18.644	2	-6.495
	2	19.148	3.878	1	-13.733	2	26.573	1	4.108
3	1	-34.029	-18.343	2	9.809	3	-23.286	2	-6.127
	2	20.310	5.260	1	-8.670	2	21.362	1	4.205
	0	22.913	0.0	0	9.878	4	8.182	3	2.484
4	1	-34.184	-18.342	2	7.282	3	-21.863	2	-6.120
	2	18.998	4.767	1	-9.300	2	21.166	1	4.207
	0	22.778	0.0	0	9.927	4	8.343	3	2.501
	3	2.337	0.651	3	-5.558	1	-8.424	4	-0.428
5	1	-34.243	-18.343	2	7.478	3	-21.813	2	-6.123
	2	18.918	4.769	1	-9.314	2	21.593	1	4.198
	0	22.724	0.0	0	9.979	4	8.195	3	2.498
	3	1.339	0.428	3	-4.986	1	-8.409	4	-0.434
	4	1.551	0.289	4	2.486	6	0.230	5	-0.012
6	1	-34.392	-18.328	2	7.506	3	-21.794	2	-6.123
	2	19.105	4.801	1	-9.327	2	21.624	1	4.200
	0	22.416	0.0	0	10.004	4	8.111	3	2.501
	3	1.724	0.484	3	-4.998	1	-8.434	4	-0.429
	4	0.921	0.178	4	2.512	6	0.169	5	0.015
	6	0.597	0.103	5	-0.675	7	0.157	6	0.015

TABLE 2.2

MINIMAX ERROR AND COMPUTATION TIME FOR DESIGN EXAMPLES

<u>R</u>	ASYMMETRIC PARTIAL RESPONSE		RAISED COSINE		SYMMETRIC PARTIAL RESPONSE		RICKER WAVELET	
	<u>ϵ</u>	<u>Time (s)</u>	<u>ϵ</u>	<u>Time (s)</u>	<u>ϵ</u>	<u>Time (s)</u>	<u>ϵ</u>	<u>Time (s)</u>
1	1.061	9.73	0.507	3.15	1.014	3.03	0.227	4.27
2	0.443	15.93	0.346	3.96	0.493	3.97	0.0897	4.69
3	0.0754	25.12	0.219	3.96	0.242	4.64	0.0159	5.66
4	0.0487	28.92	0.0965	4.60	0.00971	4.34	0.00126	5.39
5	0.0358	44.73	0.0248	4.97	0.00798	4.70	0.000931	5.58
6	0.0279	53.82	0.00067	8.32	0.00555	6.71	0.000758	9.95

2.2.3 Symmetric Partial-Response Pulse

The third example is a symmetric pulse of the partial-response type which has no spectral energy near dc. The desired impulse response samples are given by

$$d(n) = -\text{sinc}(C + 2) + 2\text{sinc}(C) - \text{sinc}(C - 2), \quad (2.9)$$

where C is defined by (2.7a) with $B = 6$. Notice from Table 2.1 that Resonator #0 was not included by the design algorithm and that the resonators were chosen in the order $\{3, 2, 4, 1, 6, 7\}$ reflecting the bandpass spectrum of this pulse.

2.2.4 Matched Filter for Ricker Wavelet

In this example it is desired to design a matched filter for a Ricker seismic wavelet [15]. The expression for the desired filter impulse response samples is

$$d(n) = \frac{\sqrt{\pi}}{2} (K - 0.5) \exp(-K), \quad (2.10)$$

where $K \triangleq [0.858\pi(2n/N-1)]^2$. Since this desired response is also symmetric, the design calculations are simplified once again as reflected in the reduced computation times given in Table 2.2.

2.3 COMPARISON OF MINIMAX AND LINPO DESIGNS

Since this study is an extension of previous work by Houts and Burlage [6] which utilized a time-domain design linear-programming algorithm Linpo, the two algorithms will be compared. The Minimax and Linpo algorithms are compared on the basis of the procedure steps outlined in Table 2.3, the features listed in Table 2.4, and

by comparing solutions to the same problem as presented in Table 2.5. The Minimax algorithm is able to solve more general problems because of the use of complex-valued coefficients. It is simpler to use because it is a three-step procedure and relies less on the user's judgement. It produces a more efficient filter because it selects the most needed resonators. In contrast, the LINPO solution for the symmetric partial-response example contained Resonators #0 and 5 even though their coefficients were essentially zero. Furthermore, the Minimax algorithm produces a filter whose impulse response is a more accurate approximation of the desired pulse.

TABLE 2.3

COMPARISON OF LINPO AND MINIMAX PROCEDURE STEPS

LINPO	MINIMAX
Determine the time interval NT for approximating the specified impulse response $d(t)$ and select either the sampling time T or the number of samples N .	Determine the time interval NT for approximating the specified impulse response $d(t)$ and select either the sampling time T or the number of samples N .
Select critical points in the pulse and specify LP objective function and set of constraints.	Determine the set of N samples $\{d(n)\}$ for the desired pulse.
Determine R based on knowledge of the pulse spectrum or by trial and error.	
Calculate $\{X(k)\}$ using Linpo (if possible). Calculate $\{h(n)\}$ and compare with desired pulse.	Calculate $\{H(k)\}$ using Minimax algorithm until either ϵ is acceptable or R reaches the allowable maximum.
If results are not satisfactory, change either the set of constraints, N , T , or R and try again.	

TABLE 2.4

COMPARISON OF LINPO AND MINIMAX FEATURES

LINPO	MINIMAX
Desired pulse shapes must be symmetric about midpoint.	Pulse symmetry is not necessary because of complex-valued filter coefficients although symmetry simplifies computations.
Filter output may not approximate desired pulse except at constrained points ($\sqrt{N/B}$).	Filter output is a minimax approximation of desired pulse over all N sample points.
Algorithm uses resonators in numerical order starting at dc, $H(0)$, and requires user to estimate the number of resonators R .	Algorithm chooses resonators in order of decreasing contribution to solution. User may specify maximum number.
Algorithm does not always produce a solution, depending on the user's choice of LP objective and constraints.	Algorithm always produces a solution although ϵ may be large.
An extra step is required to calculate $\{h(n)\}$ and determine its acceptability.	Value of ϵ after a solution is a measure of the acceptability of the approximation.

TABLE 2.5

COMPARISON OF LINPO AND MINIMAX SOLUTIONS

RAISED COSINE N = 60, R = 6			SYMMETRIC PARTIAL RESPONSE N = 50, R = 7	
k	LINPO X(k)	MINIMAX X(k)	LINPO X(k)	MINIMAX X(k)
0	10.000	10.000	0.000	----
1	-9.330	-9.327	-6.910	-7.019
2	7.500	7.506	18.090	18.025
3	-5.000	-4.998	-18.090	-18.202
4	2.500	2.512	6.867	6.798
5	-0.670	-0.675	-0.000	----
6	----	----	0.043	0.086
7	----	----	----	0.094
8	----	----	----	0.102
ϵ	0.0012	0.00067	0.0168	0.0056

CHAPTER 3

TIME-DOMAIN EQUALIZER DESIGN

This chapter deals with designing a digital equalizer to produce a specified response at the output of a known channel. The method used in this chapter is similar to that of Chapter 2 except that the channel between the equalizer and the receiver is no longer assumed to be ideally bandlimited with constant amplitude and linear phase in the passband.

3.1 THE CHANNEL MODEL

Since time-domain specifications are to be placed on the channel output, it becomes necessary to derive an expression for the channel output $y(t)$ as the convolution of the impulse responses of the channel $c_T(t)$ and equalizer $h(t)$. The digital equalizer's discrete-time output $\{h(n)\}$ can be written as a continuous-time expression using the unit impulse $\delta(t)$, i.e.,

$$h(t) = \sum_{n=0}^{N-1} h(n) \delta(t - nT). \quad (3.1)$$

Consequently, the channel output $y(t)$ is

$$\begin{aligned}
 y(t) &= \sum_{n=0}^{N-1} h(n) \int_0^t \delta(x - nT) c_T(t - x) dx \\
 &= \sum_{n=0}^{N-1} h(n) c_T(t - nT).
 \end{aligned}
 \tag{3.2}$$

The channel output is now an explicit function of the filter impulse-response samples. The channel $c_T(t)$ used in (3.2) consists of a D/A converter in cascade with a channel model $c(t)$ as shown previously in Fig. 1-1. The D/A converter is a zero-order hold with impulse response

$$g_D(t) = u(t) - u(t - T). \tag{3.3}$$

Hence, $c_T(t)$ is given by the convolution of $g_D(t)$ with $c(t)$, i.e.,

$$c_T(t) = \begin{cases} 0 & t < 0 \\ \int_0^t c(x) dx & 0 < t < T \\ \int_{t-T}^t c(x) dx & t > T. \end{cases} \tag{3.4}$$

Two channel models were used to test the time-domain equalizer design procedure. One channel model was an Mth-order lowpass filter which simulated channels with dc response, while the other was a model of a telephone channel which has a bandpass characteristic. Since the design goal was to reduce ISI in a high SNR channel, noise was not included in the design models. However, the increased noise margin as a result of channel equalization was noted. The channel models were normalized to have a break-point frequency $f_c = 1$ Hz,

which is assumed to be the Nyquist bandwidth, i.e., $1/2T_b$. Thus the minimum baud interval is $T_b = 0.5$ s.

3.1.1 Mth-Order Lowpass Filter

The first channel model is an Mth-order lowpass filter used by Houts and Burlage [6] with impulse response

$$c(t) = \frac{(2\pi)^M}{(M-1)!} t^{M-1} \exp(-2\pi t) u(t). \quad (3.5)$$

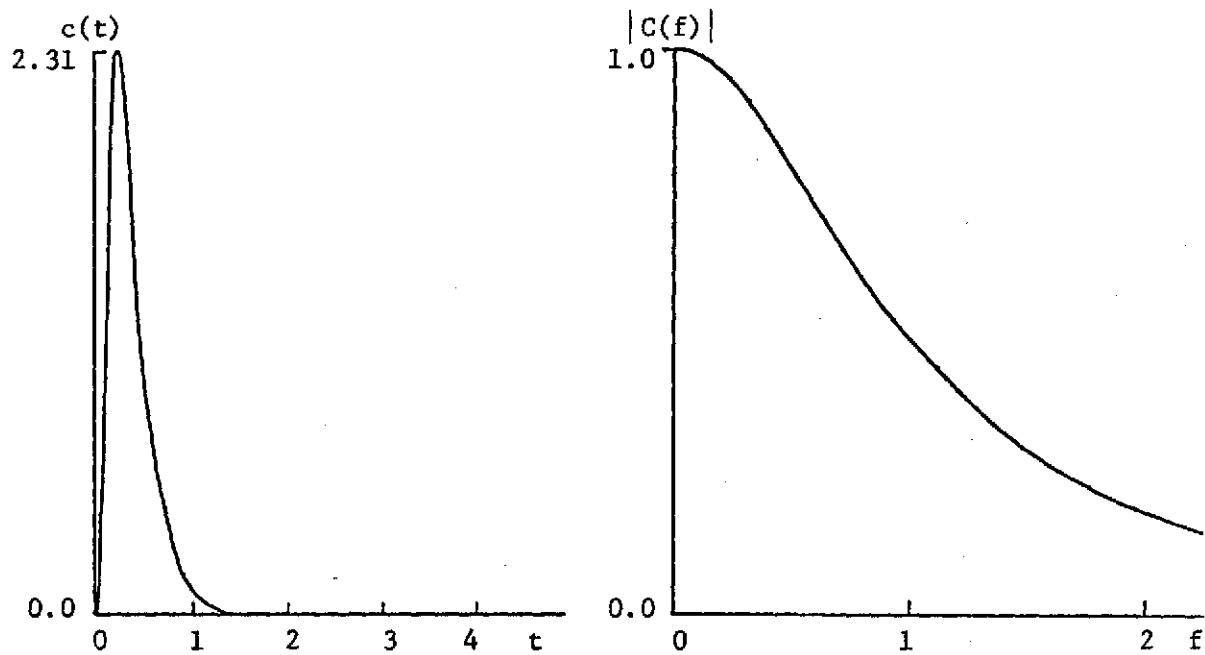
The corresponding frequency characteristic is

$$C(f) = \frac{1}{(1 + jf)^M}. \quad (3.6)$$

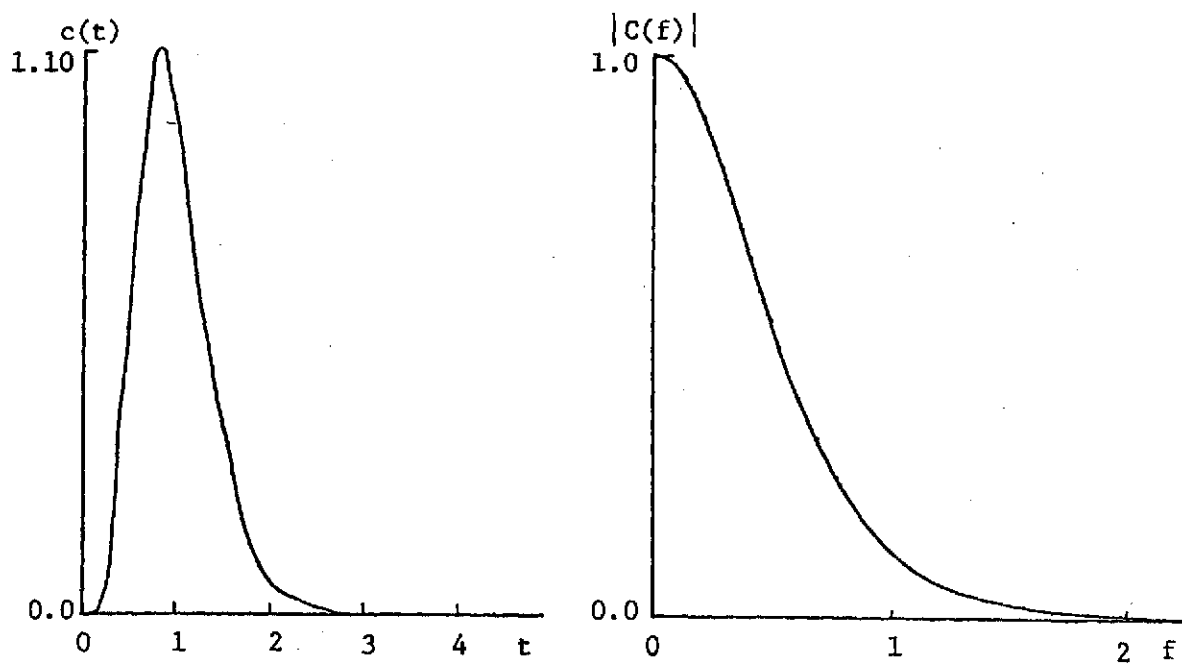
The total channel impulse response including $g_D(t)$ is

$$\begin{aligned} c_T(t) &= \int_{t-T}^t \frac{(2\pi)^M}{(M-1)!} x^{M-1} \exp(-2\pi x) u(x) dx \\ &= \left[\left[\frac{(2\pi x)^{M-1}}{(M-1)!} + \frac{(2\pi x)^{M-2}}{(M-2)!} + \dots + 1 \right] (-\exp(-2\pi x)) \right]_{\text{Max}(t-T, 0)}^{\text{Max}(t, 0)}. \end{aligned} \quad (3.7)$$

This model, although not very realistic, is included as a basis for comparison with the results of Houts and Burlage. The impulse response $c(t)$ and amplitude characteristic $|C(f)|$ of the 2nd- and 6th-order channels are given in Fig. 3-1. The impulse-response main lobes have nominal time delays T_d of 0.20 and 0.80 s respectively.



(a) 2nd-Order Channel



(b) 6th-Order Channel

Fig. 3-1. Impulse Response and Amplitude Characteristic for Mth-Order Lowpass Channel Model.

3.1.2 Telephone Channel

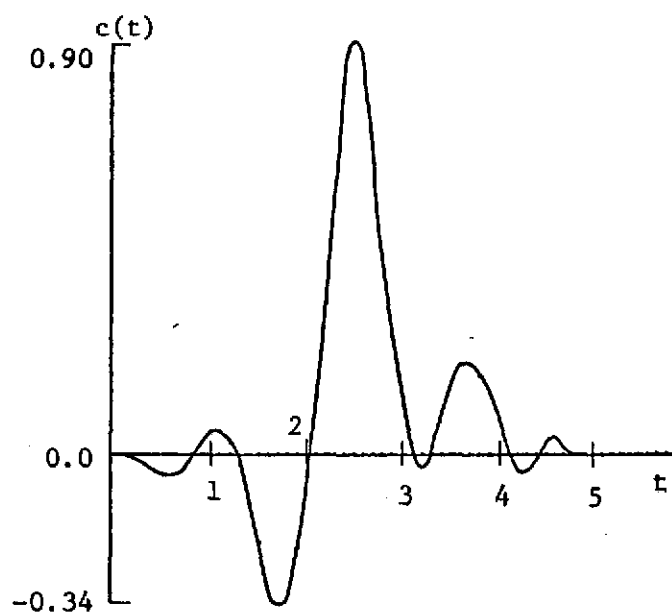
The second channel model is a more realistic model based on measurements of a 2400 baud VSB telephone channel by Westcott [19]. Values of the impulse response at baud intervals and intermediate points were taken from the measurements and used in a Spline interpolation routine [20] to produce a continuous approximation to $c(t)$. The impulse response and corresponding amplitude characteristic $|C(f)|$, which have been scaled to correspond with a 1 Hz break-point frequency, are shown in Fig. 3-2. The main lobe of the impulse response is observed to have a 2.5 s nominal time delay.

3.2 EQUALIZER DESIGN ALGORITHM

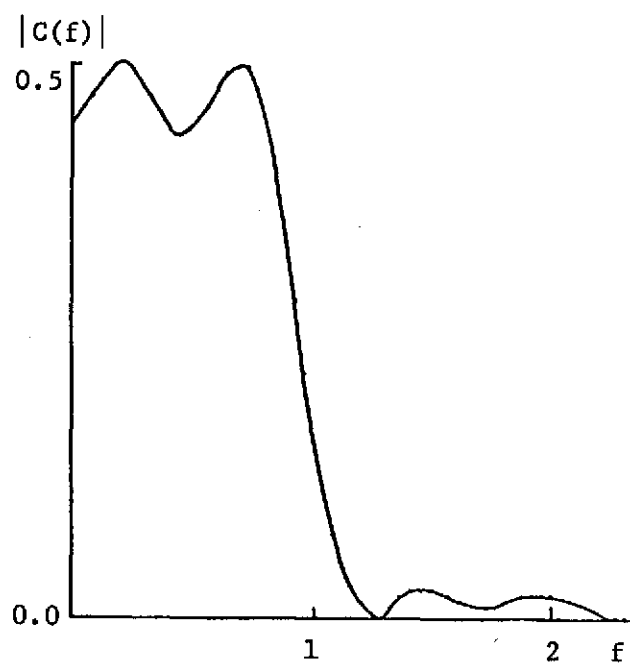
It is desired to design a FIR digital equalizer using either the transversal or frequency-sampling structure such that the channel output $y(t)$ approximates a specified pulse delayed by T_d s. The specified pulses are of the raised cosine or partial response classes, which were described in Chapter 2, and the approximation is obtained using the Minimax algorithm. The linear programming (LP) problem to be solved is a modification of (2.4), i.e.,

$$\begin{aligned}
 &\text{Minimize:} && \epsilon \\
 &\text{Subject to:} && y(nT + T_d) + \epsilon \geq d(n) \\
 & && y(nT + T_d) - \epsilon \leq d(n)
 \end{aligned}
 \quad n = 0, 1, \dots, N-1. \quad (3.8)$$

As in Chapter 2, N is the number of samples and T is the time between samples, while T_d is the nominal time delay introduced by the channel.



(a) Impulse Response



(b) Amplitude Characteristic

Fig. 3-2. Telephone Channel Model.

3.2.1 Transversal Equalizer

Using (3.2) the LP problem (3.8) can be expressed in terms of the equalizer impulse-response samples.

Minimize: ϵ

$$\text{Subject to: } \sum_{k=0}^{N-1} \left[h(k) c_T((n-k)T + T_d) \right] + \epsilon \geq d(n) \quad (3.9)$$

$$\sum_{k=0}^{N-1} \left[h(k) c_T((n-k)T + T_d) \right] - \epsilon \leq d(n)$$

$$n = 0, 1, \dots, N-1.$$

The solution to (3.9) is the set of tap gains $\{h(n)\}$ of the transversal filter. The number of constraints is restricted to 120, i.e., $N \leq 60$, because of computer core-storage limitations.

3.2.2 Frequency-Sampling Equalizer

An expression for the channel output in terms of the frequency-sampling filter coefficients can be found by substituting (1.11) into (3.2) and exchanging the order of summation.

$$\begin{aligned} y(t) = & \frac{X(0)}{N} \sum_{n=0}^{N-1} c_T(t - nT) + \frac{X(N/2)}{N} \sum_{n=0}^{N-1} (-1)^n c_T(t - nT) \\ & + \frac{2}{N} \sum_{k=1}^{N/2-1} \left[X(k) \sum_{n=0}^{N-1} \cos(2\pi kn/N) c_T(t - nT) \right. \\ & \left. - Y(k) \sum_{n=0}^{N-1} \sin(2\pi kn/N) c_T(t - nT) \right]. \end{aligned} \quad (3.10)$$

Linear programming can be employed since the output is expressed as a linear combination of the variables $X(k)$ and $Y(k)$, i.e., the real

and imaginary parts of $H(k)$ respectively. The LP problem (3.8) is solved with $y(t)$ defined by (3.10) to produce the filter coefficients $\{H(k)\}$. Recall that only R of these coefficients are allowed to have non-zero values. The iterative procedure of Section 2.1 is used to select the R resonators to be included in the solution.

3.3 DESIGN EXAMPLES FOR LOWPASS CHANNELS

Design examples using the lowpass channels of 2nd- and 6th-order are included for comparison with the Linpo-generated designs of Houts and Burlage [6]. In particular, Linpo results are compared with Minimax designs of transversal and frequency-sampling filters and a transversal design using a restricted Minimax procedure. The desired channel output is the raised-cosine pulse ($\alpha = 1$). The number of samples N is 30, and baud time T_b is 0.5 s. Note that for this baud time the nominal 1 Hz bandwidth of the channel is not adequate for the spectrum of the raised-cosine pulse since its normalized bandwidth is $(1 + \alpha)/(2T_b) = 2$ Hz. The attenuation is particularly severe for the 6th-order channel. However, this baud time value was selected in order to make the aforementioned comparison.

The Linpo and Minimax designs were compared on the basis of the number of multipliers M required in the implementation, the transmitted energy E_t , and the accuracy of the channel output. The transmitted energy is defined as the energy in the D/A converter output when a unit pulse is applied to the equalizer input, i.e.,

$$E_t = T \sum_{n=0}^{N-1} h^2(n). \quad (3.11)$$

Two accuracy criteria are used, namely the maximum error ϵ and the total peak distortion D . The maximum error ϵ is defined as the maximum absolute difference between one of N channel output samples $y(T_d + nT)$ and the corresponding desired pulse sample $d(nT)$, i.e.,

$$\epsilon \triangleq \max_{0 \leq n \leq N} |y(T_d + nT) - d(nT)|. \quad (3.12)$$

For some of the designs the difference between the channel output and the desired pulse is known only at the baud times. For these cases ϵ is the maximum difference at the baud times, i.e., replace nT in (3.12) by kT_b where $0 \leq k \leq NT/T_b$. The total peak distortion D was defined by (1.3) in terms of an infinite series; however, since the channel is causal, there is no contribution to D before time $t = 0$. Also, the channel output after time $t = T_d + 2NT$ is negligible; so D is redefined as

$$D = \sum_{n=0}^L |y(nT_b)|, \quad (3.13)$$

where

$$LT_b \leq T_d + 2NT.$$

3.3.1 Transversal Designs

The design results for the Linpo and Minimax transversal equalizers are listed in Table 3.1. The Linpo designs for the 2nd- and 6th-order channels used 12 and 15 constraint equations

TABLE 3.1

COMPARISON OF DESIGN RESULTS FOR LOWPASS CHANNELS

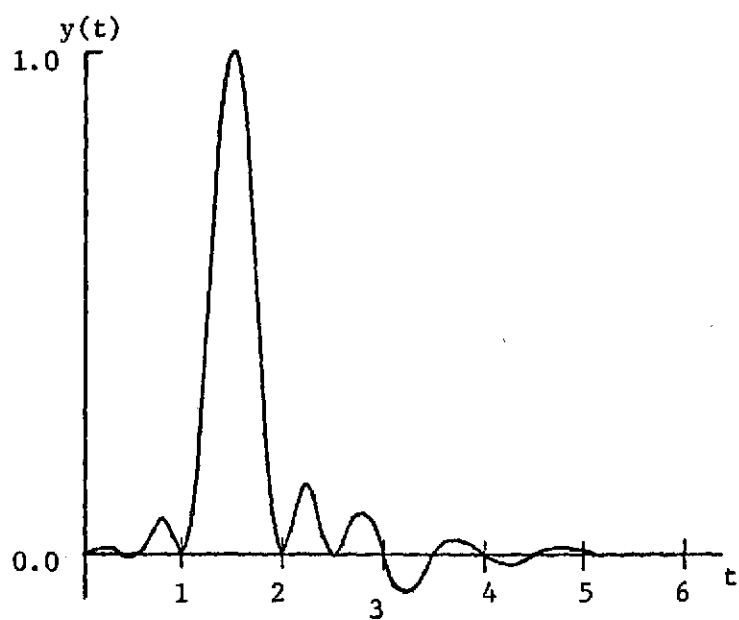
DESIGN ALGORITHM	2ND-ORDER CHANNEL				6TH-ORDER CHANNEL			
	ϵ	E_t	D	M	ϵ	E_t	D	M
Linpo Transversal	*	2.59	2.4E-9	3	*	150.1	0.015	15
Minimax Transversal	0.00011	0.74	0.0024	28	0.0017	21.4	0.025	15
Restricted-Minimax Transversal	*	2.44	0.00038	6	*	15.7	0.161	6
Linpo Frequency-Sampling	*	14.25	0.367	11	NO SOLUTION FOUND			
Minimax Frequency-Sampling	0.00033	0.73	0.0032	16	0.022	12.0	0.030	16

* $\epsilon = 0.0$ at baud times

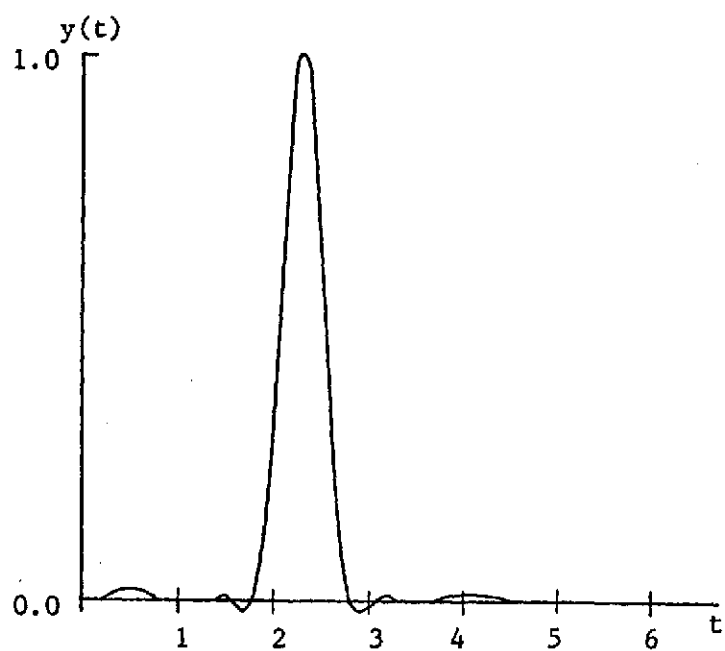
respectively. Although the design constraints were met, the resulting channel outputs were not of the raised-cosine shape. The Linpo channel output along with the Minimax channel output is shown in Fig. 3-3 for the 6th-order channel. The latter clearly has the desired raised-cosine shape. From Table 3.1 one observes that the Minimax solutions have smaller E_t values while the Linpo solution for the 2nd-order channel has fewer multipliers. In an effort to reduce the number of multipliers required, the Minimax algorithm was modified to formulate a LP problem which was similar to that of the Linpo algorithm. The constraints of (3.8) which were not at baud times were removed, and the tap gains were restricted to have alternating signs. The Linpo algorithm used alternating signs as a means of bypassing the LP restriction of non-negative variables. Predictably, these design restrictions reduced the number of multipliers M ; however, the transmitted energy E_t and total peak distortion D varied considerably. It is apparent that the Restricted-Minimax algorithm has decided advantages over both the Linpo and Minimax transversal algorithms, particularly for difficult equalization problems like the 6th-order channel example. The equalized channel has a normalized eye opening of 0.839 while requiring only 10% of the energy specified by the Linpo solution and two-fifths the number of multipliers specified by the Minimax algorithm.

3.3.2 Frequency-Sampling Designs

Frequency-sampling designs by the Minimax and Linpo algorithms are also listed in Table 3.1. However, the Linpo frequency-sampling



(a) Linpo Waveform



(b) Minimax Waveform

Fig. 3-3. Comparing Receiver Waveforms for Linpo and Minimax Transversal Equalizers with 6th-Order Channel.

algorithm is unsuitable as a tool for equalizer design because its alternating sign restriction implies the equalizer has linear phase and a symmetric impulse response. However, neither of these characteristics apply to the typical channel; consequently, it is impossible for such an equalizer to adequately compensate for the channel distortion. In fact, the Linpo algorithm could not produce a solution for the 6th-order channel example. Alternatively, the Minimax frequency-sampling algorithm produced equalizers with acceptable accuracies and smaller transmitted energies than any of the previous transversal-filter algorithms. Each channel model was compensated with a frequency-sampling equalizer using six resonators. Although these designs require 16 multipliers, Resonator #0 being first-order, the additional cost is more than offset by the reduced energy and distortion figures. Furthermore, the Minimax solution also yielded a raised-cosine output, unlike the Linpo transversal or frequency-sampling algorithms. Based on the data presented in Table 3.1, the Minimax frequency-sampling algorithm is judged to be a viable alternative to transversal designs.

3.4 COMPARISON OF FREQUENCY-SAMPLING AND TRANSVERSAL DESIGNS FOR A TELEPHONE CHANNEL MODEL

Four equalizer designs are presented in this section to demonstrate the applicability of the Minimax frequency-sampling algorithm to equalizer design for the telephone channel model described in Section 3.1.2. Results are compared with transversal equalizers designed by the Minimax and Restricted-Minimax algorithms. The criteria for comparison are once again the maximum error ϵ ,

peak distortion D , transmitted energy E_t , and number of multipliers M . The specified received-pulse waveforms are the raised cosine ($\alpha = 0,1$) and the partial response, both symmetric and asymmetric, as described in Chapter 2. For the $\alpha = 1$ raised-cosine pulse a baud time $T_b = 1.0$ s was used so that the pulse spectrum would not extend beyond 1 Hz. Similarly, $T_b = 0.5$ s represented an equivalent choice for the remaining pulses. For the raised-cosine ($\alpha = 0$) and asymmetric partial-response pulses the number of samples per baud interval B was reduced to six so that the limited number of samples available ($N = 60$) would cover more of the significant values of the pulses.

3.4.1 Frequency-Sampling Designs

The resonator coefficients for the frequency-sampling design examples are listed in Tables 3.2 and 3.3 for $R = 1,2,\dots,6$. The maximum number of resonators $R = 6$ was selected because it gave accurate results with a moderate number of multipliers. The accuracy and energy figures for the examples as well as the design calculation times are given in Table 3.4. In each design as the number of resonators increases, the maximum error ϵ decreases. The total peak distortion values compare quite favorably with $D = 0.70$ for the unequalized channel. Examination of the design results in Table 3.4 reveals that the telephone channel model can be effectively equalized using the Minimax frequency-sampling technique.

3.4.2 Transversal Designs

The results for the two transversal equalizer design techniques are given in Table 3.5. The number of multipliers for the Minimax

TABLE 3.2

FREQUENCY-SAMPLING EQUALIZER DESIGNS
FOR RAISED-COSINE PULSES ($N = 60$)

$\alpha = 1.0$ $T_b = 1.0$ $B = 10$				$\alpha = 0.0$ $T_b = 0.5$ $B = 6$			
R	k	X(k)	Y(k)	R	k	X(k)	Y(k)
1	1	-34.622	0.479	1	4	35.567	-9.582
2	1	-23.754	-14.141	2	4	15.360	2.358
	2	10.889	9.834		2	25.962	16.149
3	1	-14.563	-7.163	3	4	14.075	-2.774
	2	20.191	9.708		2	20.369	5.977
	0	24.164	0.0		1	-11.752	-5.748
4	1	-17.048	-8.292	4	4	18.272	-3.102
	2	14.234	6.968		2	16.435	5.903
	0	22.068	0.0		1	-7.217	-4.736
	3	-12.630	-2.137		3	-8.510	0.764
5	1	-16.796	-8.509	5	4	13.903	-3.206
	2	14.890	6.787		2	13.742	4.721
	0	22.060	0.0		1	-9.965	-5.693
	3	-10.896	-2.217		3	-11.611	0.154
	4	5.397	-0.823		0	13.748	0.0
6	1	-16.933	-8.537	6	4	14.050	-4.201
	2	14.737	6.731		2	12.815	4.362
	0	21.920	0.0		1	-10.701	-5.918
	3	-11.073	-2.289		3	-12.425	-0.338
	4	5.081	-0.861		0	13.034	0.0
	5	-1.304	0.001		5	-17.636	2.357

TABLE 3.3

FREQUENCY-SAMPLING EQUALIZER DESIGNS FOR
PARTIAL-RESPONSE PULSES ($B = 6$, $T_b = 0.5$)

ASYMMETRIC				SYMMETRIC			
R	k	X(k)	Y(k)	R	k	X(k)	Y(k)
1	3	-20.776	-65.241	1	2	71.001	17.249
2	3	-21.843	-39.589	2	2	52.864	18.066
	2	4.854	51.409		3	-47.284	-2.094
3	3	-7.815	-37.631	3	2	48.234	16.931
	2	6.898	39.538		3	-48.052	-1.132
	1	-11.912	-32.229		4	17.357	-5.541
4	3	-9.026	-34.788	4	2	46.569	17.263
	2	3.057	43.970		3	-45.661	0.557
	1	-8.716	-27.827		4	17.560	-4.612
	4	8.223	23.006		1	-13.817	-7.393
5	3	-8.643	-37.768	5	2	46.351	17.169
	2	3.630	41.195		3	-45.962	0.517
	1	-9.088	-29.947		4	17.221	-4.485
	4	8.512	17.222		1	-13.901	-7.519
	0	26.090	0.0		0	1.341	0.0
6	3	-8.572	-36.810	6	2	46.307	17.142
	2	3.688	41.600		3	-45.949	0.469
	1	-9.138	-29.830		4	17.389	-4.687
	4	9.227	21.264		1	-13.942	-7.531
	0	26.021	0.0		0	1.313	0.0
	5	0.099	-11.318		5	-1.447	0.554

TABLE 3.4

FREQUENCY-SAMPLING EQUALIZER DESIGN RESULTS

RAISED COSINE
 $(\alpha = 1, B = 10, T_b = 1.0)$

R	ϵ	E_t	D	TIME (s)
1	0.494	3.996	1.614	14.99
2	0.281	3.265	1.186	22.43
3	0.205	3.524	0.890	25.21
4	0.0881	3.394	0.281	34.46
5	0.0181	3.394	0.076	55.21
6	0.00511	3.395	0.0311	73.84

RAISED COSINE
 $(\alpha = 0, B = 6, T_b = 0.5)$

R	ϵ	E_t	D	TIME (s)
1	0.467	3.769	3.107	17.15
2	0.388	3.267	2.654	23.39
3	0.269	2.299	1.844	30.67
4	0.192	2.211	1.381	40.16
5	0.0972	2.155	0.958	50.54
6	0.0119	3.066	0.155	63.10

ASYMMETRIC PARTIAL RESPONSE
 $(B = 6, T_b = 0.5)$

R	ϵ	E_t	D	TIME (s)
1	1.115	13.022	1.758	16.91
2	0.799	13.086	0.595	24.68
3	0.507	11.857	1.151	30.67
4	0.246	13.004	0.158	48.91
5	0.0859	13.612	0.700	51.68
6	0.0237	14.305	0.221	64.79

SYMMETRIC PARTIAL RESPONSE
 $(B = 6, T_b = 0.5)$

R	ϵ	E_t	D	TIME (s)
1	0.935	14.829	4.840	18.34
2	0.4302	14.892	1.378	26.95
3	0.2206	14.599	1.438	34.39
4	0.0167	14.242	0.176	52.53
5	0.00866	14.232	0.188	52.59
6	0.00267	14.246	0.114	62.22

TABLE 3.5

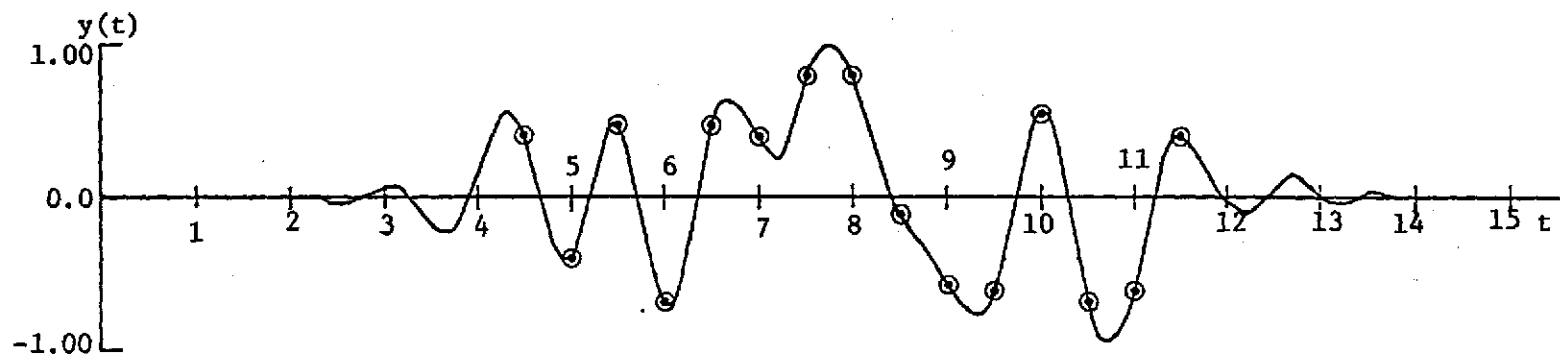
TRANSVERSAL EQUALIZER DESIGNS

ALGORITHM	RAISED COSINE ($\alpha = 1, B = 10, T_b = 1.0$)				
	M	ϵ	E_t	D	Time (s)
Minimax	27	0.000675	6.138	0.0128	234.34
Restricted Minimax	6	0.532	11.147	0.0180	4.27
	RAISED COSINE ($\alpha = 0, B = 6, T_b = 0.5$)				
	M	ϵ	E_t	D	Time (s)
Minimax	29	0.000587	5.304	0.136	245.36
Restricted Minimax	10	0.0930	14.519	0.0620	5.42
	ASYMMETRIC PARTIAL RESPONSE ($B = 6, T_b = 0.5$)				
	M	ϵ	E_t	D	Time (s)
Minimax	32	0.00105	31.834	0.105	298.72
Restricted Minimax	10	0.202	79.617	0.0963	5.44
	SYMMETRIC PARTIAL RESPONSE ($B = 6, T_b = 0.5$)				
	M	ϵ	E_t	D	Time (s)
Minimax	26	0.00130	30.821	0.0996	220.65
Restricted Minimax	10	0.176	79.408	0.158	5.57

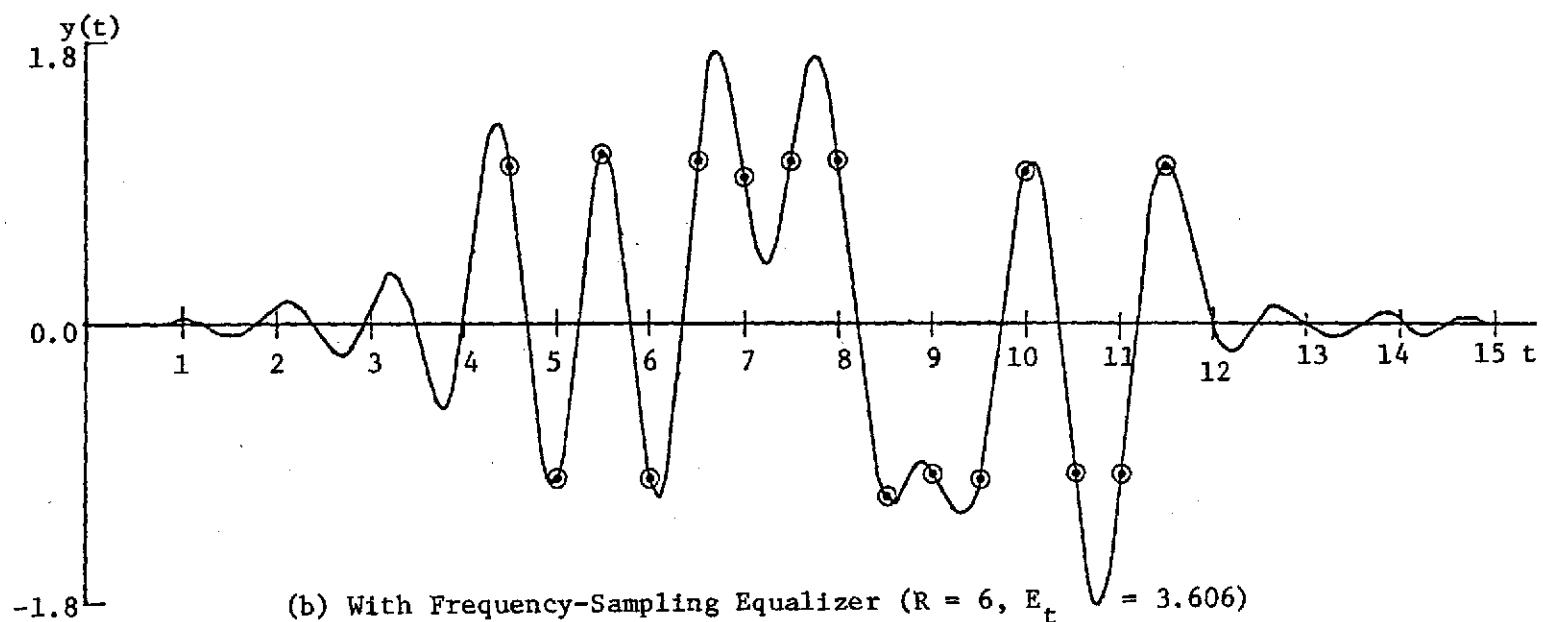
designs range from 26 to 32, and the required energy E_t is approximately twice that of the corresponding frequency-sampling equalizer. Although the Restricted-Minimax transversal equalizer designs use fewer multipliers, the required energy is increased considerably over its frequency-sampling counterpart without improving the accuracy. Consequently, the frequency-sampling equalizer is judged to be superior to the transversal equalizer designs.

3.5 EXAMPLE OF EQUALIZED DATA TRANSMISSION

Data transmission through the telephone channel was simulated by a 15 bit pseudo-noise (PN) sequence both with and without equalization. For the unequalized case a sequence of samples, each with an energy E_t and spaced 0.5 s apart, were applied to the channel input. For the equalized case the data was represented by positive and negative unit pulses, spaced 0.5 s apart, applied to the equalizer input. The raised-cosine ($\alpha = 0$) equalizer design was used with $N = 40$ and $B = 5$. The energy in the equalizer impulse response was E_t . The channel outputs for both cases are shown in Fig. 3-4. Notice that equalization has greatly increased the noise margin in this example. The increase in normalized eye opening from 0.120 to 0.933 represents a 17.8 dB SNR improvement.



(a) No Equalizer ($E_t = 3.606$)



(b) With Frequency-Sampling Equalizer ($R = 6$, $E_t = 3.606$)

Fig. 3-4. Effect of Minimax Designed Equalizer on 15 Bit PN Sequence Transmitted Over Telephone Channel.

CHAPTER 4

ENERGY-MINIMIZATION EQUALIZER DESIGN

The design of an equalizer in which ISI is constrained to a given maximum level and transmitted energy is minimized is presented in this chapter. For ISI-free transmission the composite frequency characteristic of the transmitted pulse and channel must meet the Nyquist criterion. This means that much of the transmitted energy is forced through the channel at frequencies where the attenuation is high in order to produce an overall flat spectrum for a bandwidth W Hz. However, if a small amount of ISI were allowed, the transmitted energy could be reduced.

4.1 ENERGY MINIMIZATION DESIGN

The Energy-Minimization design algorithm minimizes the transmitted energy for a given ϵ and some associated distortion D . The channel output is constrained to not differ from the specified waveform more than ϵ for samples taken at the baud times.

4.1.1 Transversal Equalizer

The energy in the D/A converter output when a unit pulse is applied to the equalizer is

$$E_t = T \sum_{n=0}^{N-1} h^2(n), \quad (4.1)$$

where $\{h(n)\}$ is the set of transversal filter impulse-response samples or tap gains. The channel output constraints can also be written in terms of the impulse-response samples using (3.2). Since the energy function is quadratic and the output constraints are linear, the energy minimization can be expressed as a quadratic programming problem.

$$\begin{aligned} \text{Minimize: } & E_t \\ \text{Subject to: } & y(nT_b + T_d) + \epsilon \geq d(nB) \\ & n = 0, 1, \dots, N/B. \\ & y(nT_b + T_d) - \epsilon \leq d(nB) \end{aligned} \quad (4.2)$$

The set $\{d(nB)\}$ is the set of samples for the specified received waveform taken at its zero crossings and/or baud times.

4.1.2 Frequency-Sampling Equalizer

The energy in the impulse response of the frequency-sampling equalizer in cascade with the D/A converter can be expressed in terms of the resonator coefficients by using (1.11) with (4.1).

$$E_t = \frac{T}{N} \left[X^2(0) + X^2(N/2) + 2 \sum_{k=1}^{N/2-1} [X^2(k) + Y^2(k)] \right]. \quad (4.3)$$

As in the transversal case this function is quadratic, and the energy minimization is achieved using the quadratic programming problem (4.2) with the channel output $y(t)$ defined by (3.10).

The selection of which resonators to include in the design is not

so straight forward as in the Minimax algorithm. There is no error waveform $\{e(nT)\}$ whose frequency components are related to the most needed resonators. The choice can be made by a search based on knowledge of the spectra of the desired pulse and channel. However, in this chapter the resonators used in the examples are the same as those of the corresponding examples of Chapter 3. This choice of resonators will give a fair comparison of the Minimax and Energy-Minimization algorithms.

4.2 DESIGN EXAMPLES

Energy-Minimization designs of transversal and frequency-sampling equalizers are compared with Minimax transversal and frequency-sampling designs based on the number of multipliers M , the transmitted energy E_t , and the accuracy criteria (D and ϵ) discussed in Section 3.3. The specified channel outputs are the raised-cosine ($\alpha = 0,1$) and partial-response (asymmetric and symmetric) pulses used in earlier comparisons. Each of these pulses has constraint equations specified at time samples corresponding to zero crossings and/or baud times for use in (4.2), the Energy-Minimization program. The time points and the pulse values at the points are tabulated in Table 4.1.

4.2.1 Transversal Designs

The transversal equalizers are designed using $N = 30$, i.e., the number of multipliers $M \leq 30$. Design results for the four aforementioned waveforms are found in Table 4.2, where the channel is the telephone channel model described in Section 3.1.2.

TABLE 4.1

CONSTRAINT POINTS FOR ENERGY-MINIMIZATION DESIGNS

RAISED COSINE, $\alpha = 1$		RAISED COSINE, $\alpha = 0$	
t	$d(t + T_d)$	t	$d(t + T_d)$
0.0	0.0	0.0	0.0
0.5	0.0	0.5	0.0
1.0	0.0	1.0	0.0
1.5	0.0	1.5	0.0
2.0	0.0	2.0	0.0
3.0	1.0	2.5	1.0
4.0	0.0	3.0	0.0
4.5	0.0	3.5	0.0
5.0	0.0	4.0	0.0
5.5	0.0	4.5	0.0
6.0	0.0	5.0	0.0

ASYMMETRICAL PARTIAL RESPONSE		SYMMETRICAL PARTIAL RESPONSE	
t	$d(t + T_d)$	t	$d(t + T_d)$
0.0	0.0	0.0	0.0
0.5	0.0	0.5	0.0
1.0	0.0	1.0	0.0
1.5	0.0	1.5	-1.0
2.0	2.0	2.0	0.0
2.5	1.0	2.5	2.0
3.0	-1.0	3.0	0.0
3.5	0.0	3.5	-1.0
4.0	0.0	4.0	0.0
4.5	0.0	4.5	0.0
5.0	0.0	5.0	0.0

TABLE 4.2

COMPARISON OF TRANSVERSAL EQUALIZER DESIGN EXAMPLES

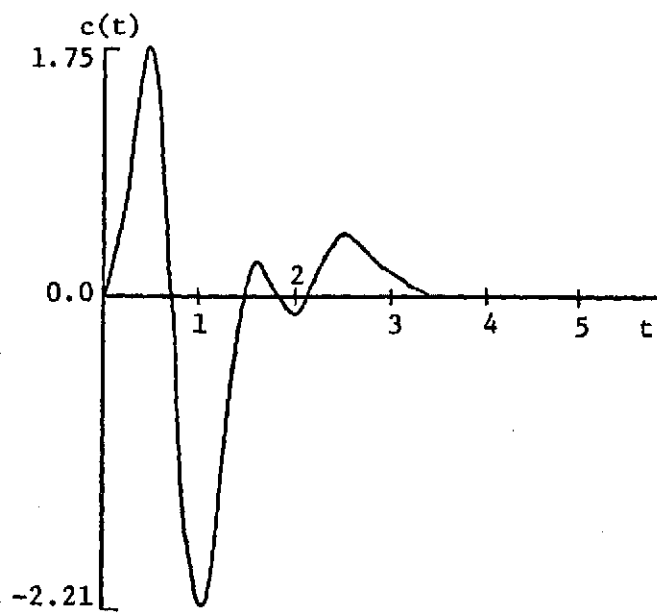
CHANNEL OUTPUT PULSE	DESIGN ALGORITHM	ϵ	E_t	D	TIME (s)
Raised Cosine $\alpha = 1$	Minimax	5.49×10^{-8}	3.405	0.0109	49.35
	Energy Minimization	4.47×10^{-8}	2.691	0.0238	171.83
Raised Cosine $\alpha = 0$	Minimax	1.68×10^{-7}	3.203	0.138	42.59
	Energy Minimization	4.00×10^{-3}	2.858	0.131	189.04
Partial Response Symmetric	Minimax	3.35×10^{-7}	14.251	0.0928	46.95
	Energy Minimization	2.98×10^{-8}	14.196	0.0946	247.15
Partial Response Asymmetric	Minimax	3.28×10^{-7}	14.330	0.112	48.50
	Energy Minimization	5.00×10^{-4}	14.174	0.110	247.41

Corresponding results for the Minimax transversal equalizer are included for comparison. It is significant to note that for every example the Energy-Minimization design yielded a smaller transmitted energy at the cost of a considerable increase in computer time. Two of the example pulses were more difficult to equalize, i.e., the Minimax designs had $D > 0.1$. However, the Energy-Minimization designs for these examples yielded slightly lower total peak distortions.

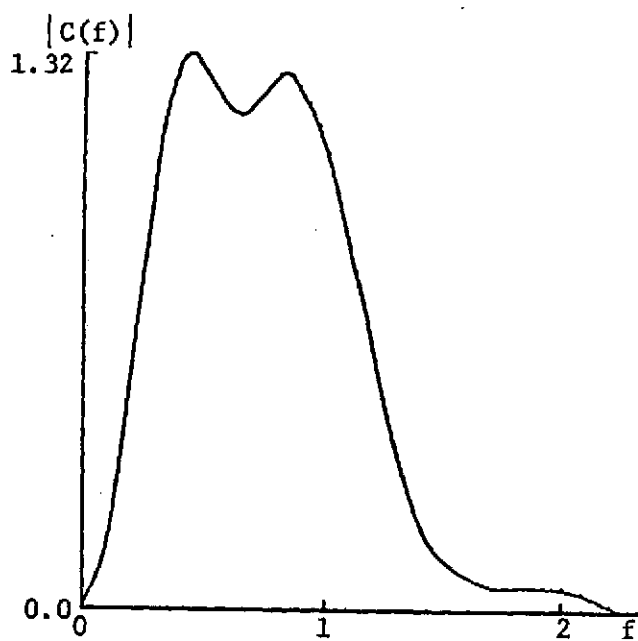
4.2.2 Frequency-Sampling Designs

Two channel models are used for the frequency-sampling examples. One is the aforementioned telephone channel model, and the other is a 6-pole bandpass filter (BPF) with bandedges of 300 and 3400 Hz. The impulse response for the bandpass filter was derived from measurements of the cross-correlation with white noise for 100 points [21]. These data values were connected to form a continuous function using Spline interpolation [20], and the time interval was scaled to correspond to a BPF with an upper bandedge of 1 Hz. The impulse and amplitude response of this BPF channel model are given in Fig. 4-1.

The results for Minimax and Energy-Minimization designs of frequency-sampling equalizers using six resonators ($M = 16$) are listed in Tables 4.3 and 4.4. Notice that in almost all cases the Energy-Minimization design has smaller ϵ , E_t , and D , and requires less computation time. Since the Energy-Minimization algorithm places fewer constraints on the channel output waveform, its channel output may not approximate the specified



(a) Impulse Response



(b) Amplitude Characteristic

Fig. 4-1. Bandpass Filter Channel Model.

TABLE 4.3

COMPARISON OF FREQUENCY-SAMPLING EQUALIZER
DESIGN EXAMPLES FOR TELEPHONE CHANNEL

CHANNEL OUTPUT PULSE	DESIGN ALGORITHM	ϵ	E_t	D	TIME (s)
Raised Cosine $\alpha = 1$	Minimax	0.00511	3.395	0.0311	73.84
	Energy Minimization	0.00400	3.382	0.0292	38.22
Raised Cosine $\alpha = 0$	Minimax	0.0119	3.066	0.115	63.10
	Energy Minimization	0.00400	2.885	0.114	36.71
Partial Response Symmetric	Minimax	0.00267	14.246	0.114	62.22
	Energy Minimization	0.00200	14.198	0.113	51.60
Partial Response Asymmetric	Minimax	0.0237	14.305	0.221	64.79
	Energy Minimization	0.0150	14.184	0.219	45.33

TABLE 4.4

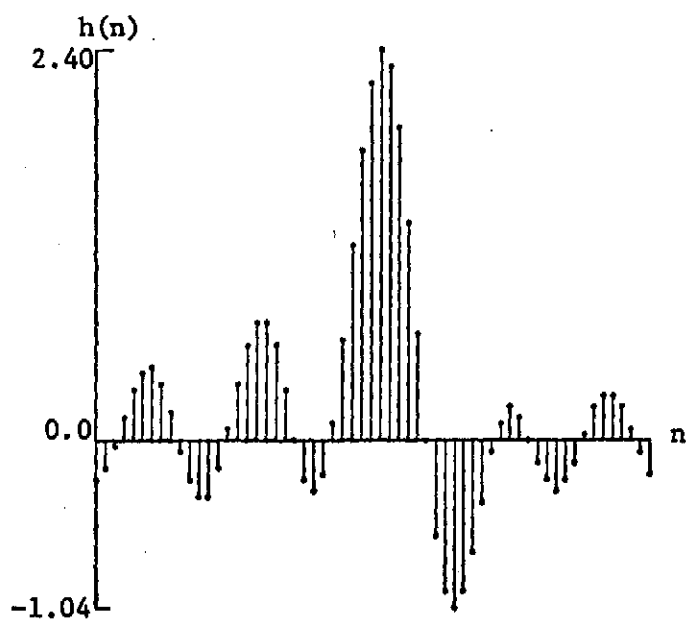
COMPARISON OF FREQUENCY-SAMPLING EQUALIZER
DESIGN EXAMPLES FOR BPF CHANNEL

CHANNEL OUTPUT PULSE	DESIGN ALGORITHM	ϵ	E_t	D	TIME (s)
Raised Cosine $\alpha = 1$	Minimax	0.0798	7.632	0.510	73.47
	Energy Minimization	0.0640	7.497	0.531	36.40
Raised Cosine $\alpha = 0$	Minimax	0.0322	2.116	0.676	61.37
	Energy Minimization	0.0300	1.765	0.631	54.04
Partial Response Symmetric	Minimax	0.0200	2.290	0.233	64.34
	Energy Minimization	0.0100	2.236	0.220	40.26
Partial Response Asymmetric	Minimax	0.154	7.312	1.591	65.95
	Energy Minimization	0.100	6.361	1.175	46.63

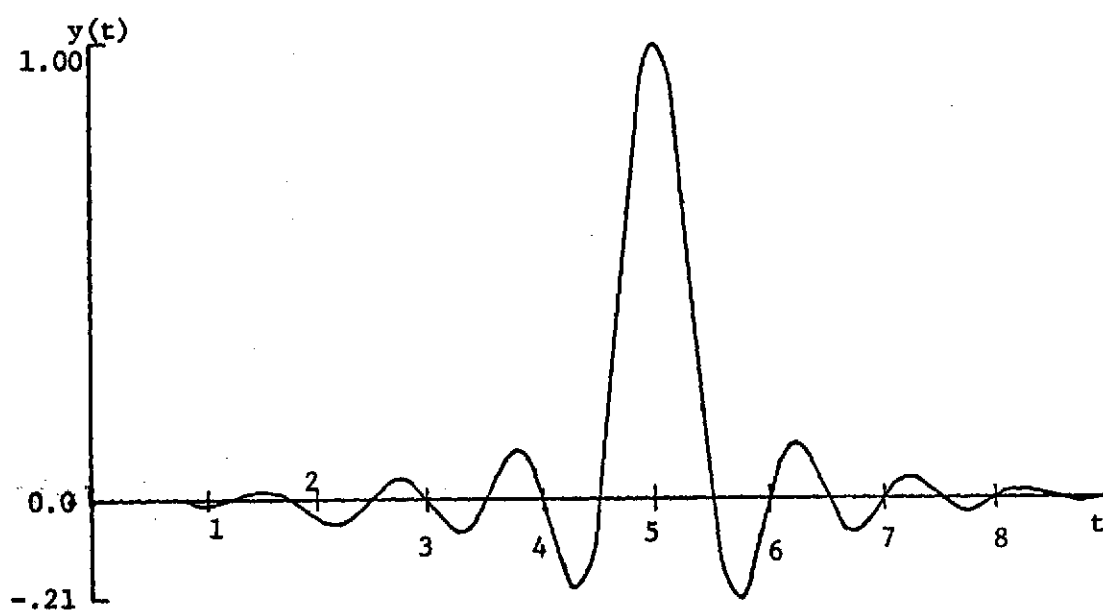
pulse as closely as the Minimax design. However, the small difference allows the Energy-Minimization designs to achieve lower ISI with less transmitted energy. The equalizer impulse response and the channel output for the Energy-Minimization design using the raised cosine ($\alpha = 0$) specification and the telephone channel model is given in Fig. 4-2.

4.2.3 Distortion vs. Energy Trade-off

The values of ϵ needed by the Energy-Minimization algorithm for both transversal and frequency-sampling designs were chosen by successive approximation. Further, the choice of ϵ gives the designer a trade-off parameter between D , the level of ISI in the received signal, and E_t , the energy in the transmitted signal. By a proper choice of ϵ based on the design considerations of a particular communication system, its error performance can be enhanced. As an illustration the frequency-sampling equalizer design for raised cosine ($\alpha = 0$) using the BPF channel model was run for several values of ϵ , and the results plotted in Fig. 4.3. As ϵ was increased, E_t was reduced at the cost of increased distortion D . As ϵ was reduced the opposite occurred. The isolated point represents the ϵ , E_t , and D values for the Minimax design. Notice that the E_t and D curves cross below this point. Based upon the results presented in this section, it is concluded that while the Minimax algorithm produces useful designs, for many specified outputs and channels the Energy-Minimization algorithm will produce designs with both lower distortion and transmitted energy.



(a) Frequency-Sampling Equalizer Impulse Response



(b) Telephone Channel Output (\sim Raised Cosine, $\alpha = 0$)

Fig. 4-2. Time-Domain Responses for Energy-Minimization Algorithm.

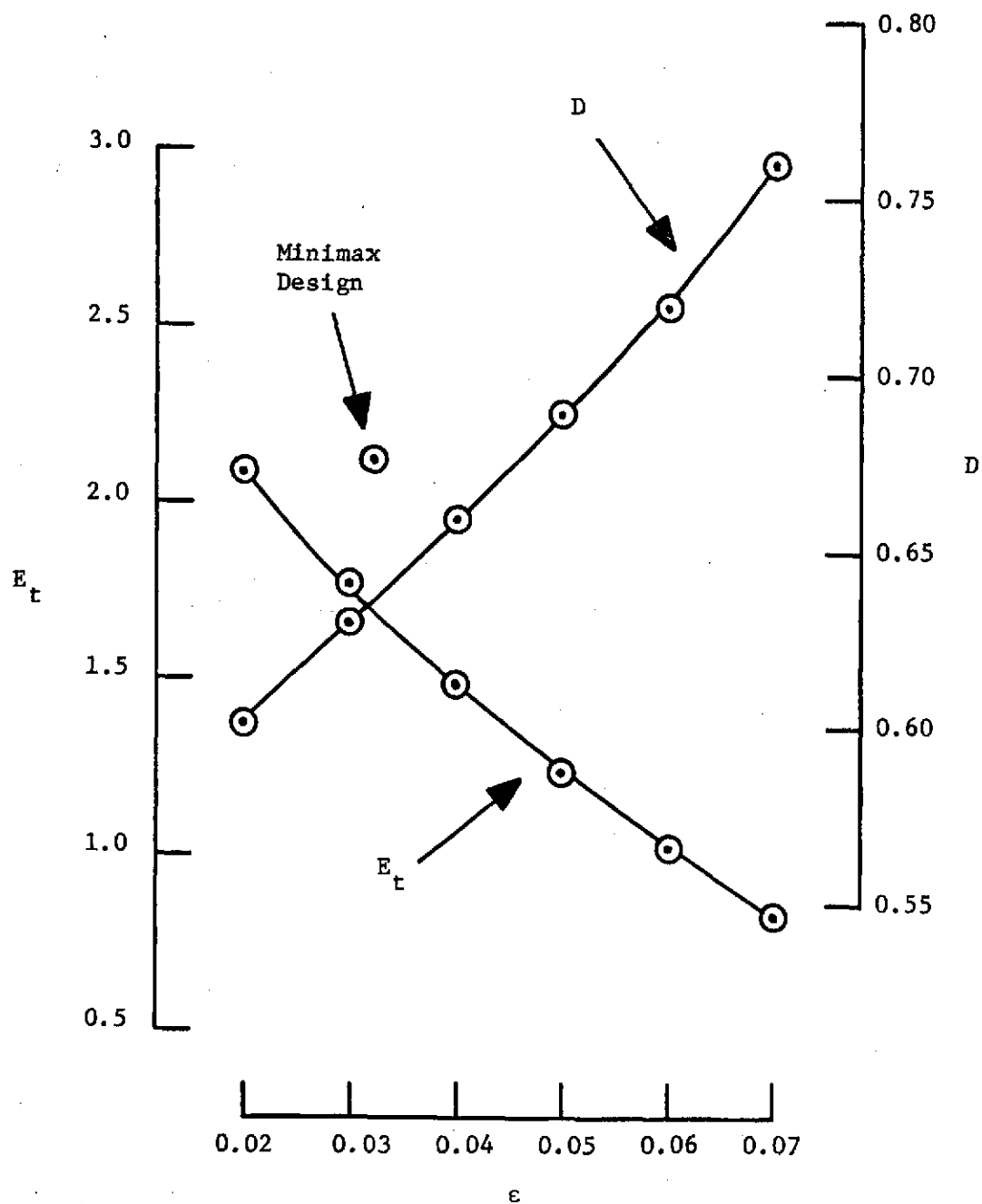
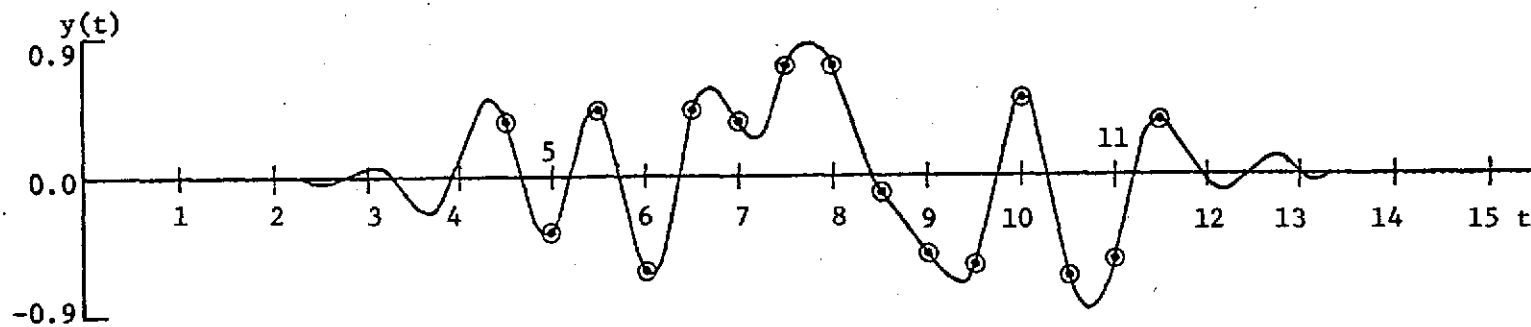


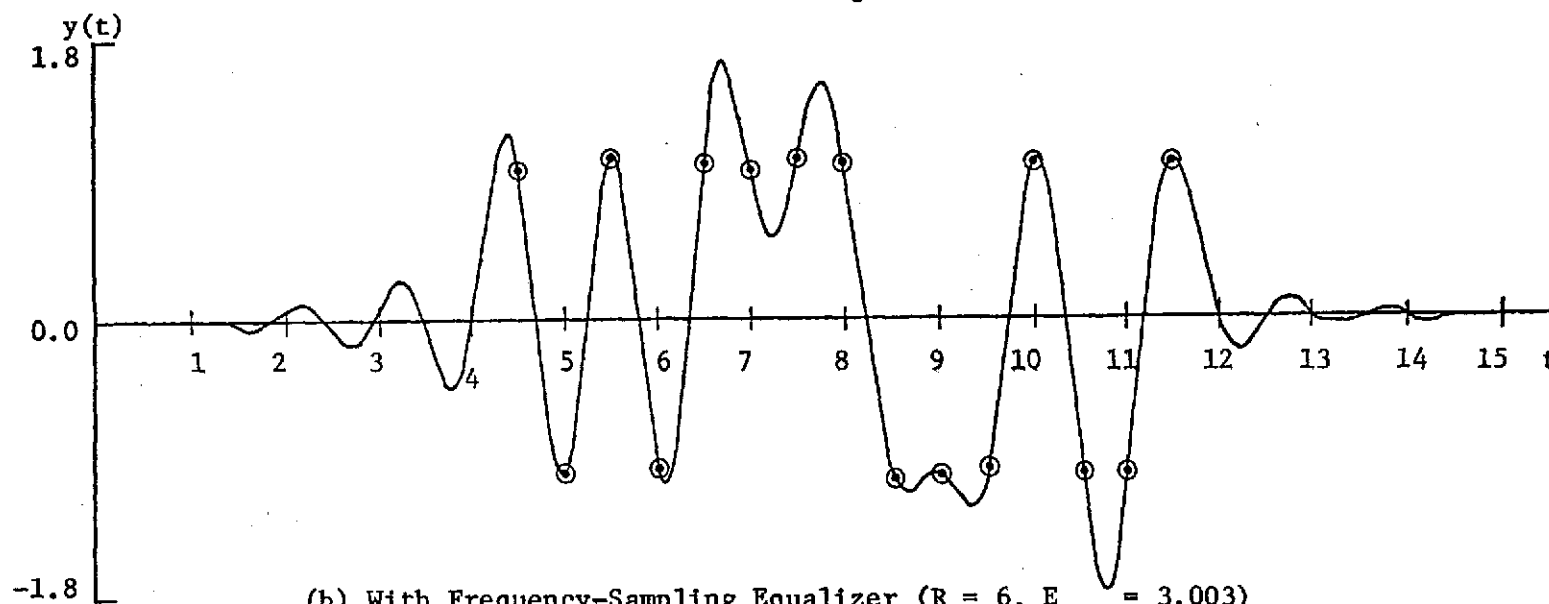
Fig. 4-3. Compromise Between ISI and Transmitted Energy by the Selection of ϵ .

4.3. EXAMPLE OF EQUALIZED DATA TRANSMISSION

Data transmission through the telephone channel was simulated by a 15 bit PN sequence as discussed previously in Section 3.5. For the unequalized case a sequence of samples of energy E_t was applied to the channel input, while for the equalized case the data were represented by positive and negative unit pulses applied to the equalizer input. The Energy-Minimization design with the raised cosine ($\alpha = 0$) specification was used. For both cases $T_b = 0.5$, $N = 40$, $B = 5$, and the energy input per bit to the telephone channel was E_t . The channel outputs are given in Fig. 4-4. The effect of equalization is an even greater increase in the noise margin than that using the Minimax-designed equalizer. The increase in normalized eye opening from 0.110 to 0.955 represents an 18.8 dB SNR improvement as compared with the 17.8 dB improvement for the Minimax design.



(a) No Equalizer ($E_t = 3.003$)



(b) With Frequency-Sampling Equalizer ($R = 6$, $E_t = 3.003$)

Fig. 4-4. Effect of Energy-Minimization Designed Equalizer on 15 Bit PN Sequence Transmitted Over Telephone Channel.

CHAPTER 5

SUMMARY AND RECOMMENDATIONS

The basic effort of this study was to develop design algorithms for FIR digital filters which could effectively be used for pulse shaping and channel equalization. In Chapter 2 the Minimax algorithm was developed to design a frequency-sampling filter with an impulse response which approximated a specified impulse response in a minimax sense. No restrictions of symmetry were placed on the filter impulse response since the generated resonator coefficients were complex-valued. Also, the algorithm produced an efficient filter by selecting the resonators to include in the design according to their contribution to the filter output. The applications given for such filters were equalization of an unknown channel, assumed ideal bandlimited, and matched filter reception. It was demonstrated that a frequency-sampling filter with only a small number of resonators could accurately approximate the specified impulse response. Further, the Minimax algorithm was compared with the Linpo algorithm, a design procedure by Houts and Burlage [6]. The advantages of the Minimax algorithm are listed in Table 2.4.

In Chapter 3 the Minimax algorithm was extended to design transversal and frequency-sampling equalizers for known but not ideal channels. The comparison of Minimax and Linpo designs using

lowpass channel models showed that the Minimax designs produced accurate approximations of the specified pulse with much less transmitted energy. Transversal and frequency-sampling filter designs by the Minimax algorithm were also compared using a telephone channel model with the transversal designs being more accurate inside the approximation interval. However, the frequency-sampling designs had lower transmitted energy and total peak distortion figures. The designs would have been equivalent if the frequency-sampling designs had included all $N/2 + 1$ resonators. The price paid for including only six was slightly larger minimax error inside the approximation interval, but the benefits were a smaller transmitted energy and less ISI outside the approximation interval.

In Chapter 4 a design algorithm was developed which minimized the transmitted energy while constraining the maximum error ϵ at any sampling point. This Energy-Minimization algorithm was compared to the Minimax algorithm for both transversal and frequency-sampling equalizers. Most of the Energy-Minimization designs required less transmitted energy and provided lower total peak distortion than the corresponding Minimax designs. Also, the specification of ϵ provided a means of compromise between the energy required and the resultant distortion in the received waveform.

A recommended area for further research is the modification of the Energy-Minimization design algorithm for frequency-sampling equalizers to include a better method of resonator selection. Since there is no error signal whose frequency components could

be related to the needed resonators as in the Minimax algorithm, the choice of which resonators to include in the design is not so straightforward. Possibly an iterative procedure using the value of the channel output at the constraint points could be investigated.

APPENDIX A

OPTIMIZATION AND FFT PROGRAMS

The optimization and FFT subroutines used in the Minimax and Energy-Minimization algorithms are discussed in this section. The optimization techniques are linear and quadratic programming. Brief explanations of the three subroutines are given with emphasis on their applicability to digital filter design. Further information can be found in the literature [22-24].

A.1 REVISED-SIMPLEX LINEAR PROGRAMMING

The linear programming (LP) problem is to minimize an objective function Z which is linear in the N unknown variables $\{x(n)\}$ subject to a set of M linear constraints.

$$\begin{aligned} \text{Minimize: } Z &= \sum_{n=1}^N p(n) x(n), \\ \text{Subject to: } \sum_{n=1}^N a(m,n) x(n) &= b(m) \quad m = 1, 2, \dots, M \\ x(n) &\geq 0 \quad n = 1, 2, \dots, N. \end{aligned} \tag{A.1}$$

It is possible to express a constraint set containing inequality constraints in the form of (A.1) by adding additional variables. It is also possible to use LP to solve a problem with unrestricted

variables. Let the original variables be $\{y(n)\}$, $n = 1, \dots, N/2$. These are written as differences of the N non-negative variables $\{x(n)\}$, i.e.,

$$y(n) = x(n) - x(n + N/2) \quad n = 1, \dots, N/2. \quad (A.2)$$

The basic computational tool used to solve the LP problem is the Simplex method which examines a sequence of feasible solutions to (A.1), each one with a smaller Z , which terminates with the minimum Z if one exists. To each solution there corresponds a basis matrix \underline{B} , i.e., a set of linearly independent columns of \underline{A} , the matrix whose elements are $\{a(m,n)\}$. The variables whose columns are in \underline{B} have non-zero values while all other variables are zero. The technique adds and removes variables from the basis in moving from one feasible solution to the next by pivoting. The variable to be added or removed is selected according to its contribution to improving the solution.

The Revised Simplex method performs the same functions as the original simplex, yet it has several advantages. In the Revised Simplex method all the information needed to proceed from one solution to the next is calculated using \underline{B}^{-1} . Thus pivoting involves only the columns in \underline{B} rather than all those in \underline{A} , and the required computer storage is reduced. Also, for LP problems with a large number of zero elements in \underline{A} , the number of computations is reduced. In addition, at any solution step the accuracy lost because of roundoff error can be restored by reinverting the basis. The Revised Simplex program used for this

study was SIMPDX, a FORTRAN subroutine written by Diderrich [25]. It was chosen because it quickly and accurately solved the large LP problems necessary for the Minimax design algorithm.

A.2 QUADRATIC PROGRAMMING USING THE WOLFE METHOD

The quadratic programming (QP) problem is to minimize an objective function which is quadratic in the unknown variables subject to a set of linear constraints.

$$\begin{aligned}
 \text{Minimize: } & \sum_{n=1}^N p(n) x(n) + \frac{1}{2} \sum_{n=1}^N \sum_{k=1}^N x(n) q(n,k) x(k), \\
 \text{Subject to: } & \sum_{n=1}^N a(m,n) x(n) = b(m) \quad m = 1, \dots, M \\
 & x(n) \geq 0 \quad n = 1, \dots, N.
 \end{aligned} \tag{A.3}$$

Inequality constraints and unrestricted variables can be incorporated in (A.3) in similar manner as for the LP problem. If the matrix Q , whose elements are $\{q(n,k)\}$, is positive definite, satisfaction of the Kunn-Tucker conditions [26] is necessary and sufficient for a solution to (A.3). These conditions are satisfied by a solution to (A.4).

$$\begin{aligned}
 \sum_{k=1}^N a(m,k) x(k) &= b(m) \quad m = 1, 2, \dots, M \\
 \sum_{k=1}^N q(n,k) x(k) + \sum_{k=1}^M a(k,n) \lambda(k) + y(n) &= -p(n) \quad n = 1, 2, \dots, N
 \end{aligned} \tag{A.4}$$

where

$$\begin{aligned}x(n) &\geq 0 \\y(n) &\leq 0 \\x(n) y(n) &= 0 .\end{aligned}$$

Problem (A.4) can be solved using a modified Simplex procedure due to Wolfe [27]. The Simplex method is used to find a feasible solution to (A.4) with the restriction that only one of the variables $x(n)$ or $y(n)$ may be in the basis at a time. The FORTRAN subroutine WOLFE used in the Energy-Minimization algorithm was written using information in References 23, 26, 27. It uses a dual Simplex technique to obtain primal feasibility and an artificial variables technique to solve (A.4).

A.3 FAST FOURIER TRANSFORM

The fast Fourier transform (FFT) is a rapid computational algorithm for calculating the discrete Fourier transform (DFT) of a sequence of samples. The DFT transform pair is

$$\begin{aligned}X(k\Delta f) &= \sum_{n=0}^{N-1} x(n\Delta t) \exp(-j2\pi kn/N) \\x(n\Delta t) &= \frac{1}{N} \sum_{k=0}^{N-1} X(k\Delta f) \exp(j2\pi kn/N),\end{aligned}\tag{A.5}$$

where N is the number of time or frequency samples and

$$T = N\Delta t = N/F = 1/\Delta f.\tag{A.6}$$

Calculation of the DFT using (A.5) requires N^2 complex multiplications. With the FFT this number can be reduced to $N \cdot \log_2(N)$ allowing the DFT to be calculated in less time and with less error [24]. The computational savings of the FFT result from dividing the problem into a large number of DFT's each with a small number of points. The greatest savings are realized when N contains many prime factors. The figures above are for N equal a power of two. The FFT program used in the Minimax algorithm was FOURT, a FORTRAN subroutine written by Brenner [28]. This program was chosen because it is a general algorithm not requiring N to be a power of two but providing as much computational savings as possible depending on the prime factors of N .

APPENDIX B

DESIGN PROGRAMS

The five main programs used to accomplish the filter designs in Chapters 2, 3, and 4 are described in Section B.1. Several subprograms are called by the main design programs including SIMPDX, WOLFE, and FOURT which are discussed in App. A. The remaining subprograms and their functions are listed in Section B.2. Source listings of the main programs and subprograms can be found in Reference 29.

B.1 MAIN DESIGN PROGRAMS

The Minimax designs of pulse shaping filters for an ideal channel in Chapter 2 were performed by the FORTRAN main program PSIC. The Minimax design algorithm of Chapter 3 for a realistic channel was implemented by PSRCT and PSRCF (T and F signify transversal or frequency-sampling). The programs EMRCT and EMRCF performed the Energy-Minimization designs of Chapter 4. Each of these five programs is described by a flowchart in Fig. B-1 through Fig. B-5. The input data needed by these programs is a description of the design problem and is listed in Table B.1. The output produced by the programs includes the design results, the accuracy and energy measures, the filter impulse response, and the channel output (if applicable).

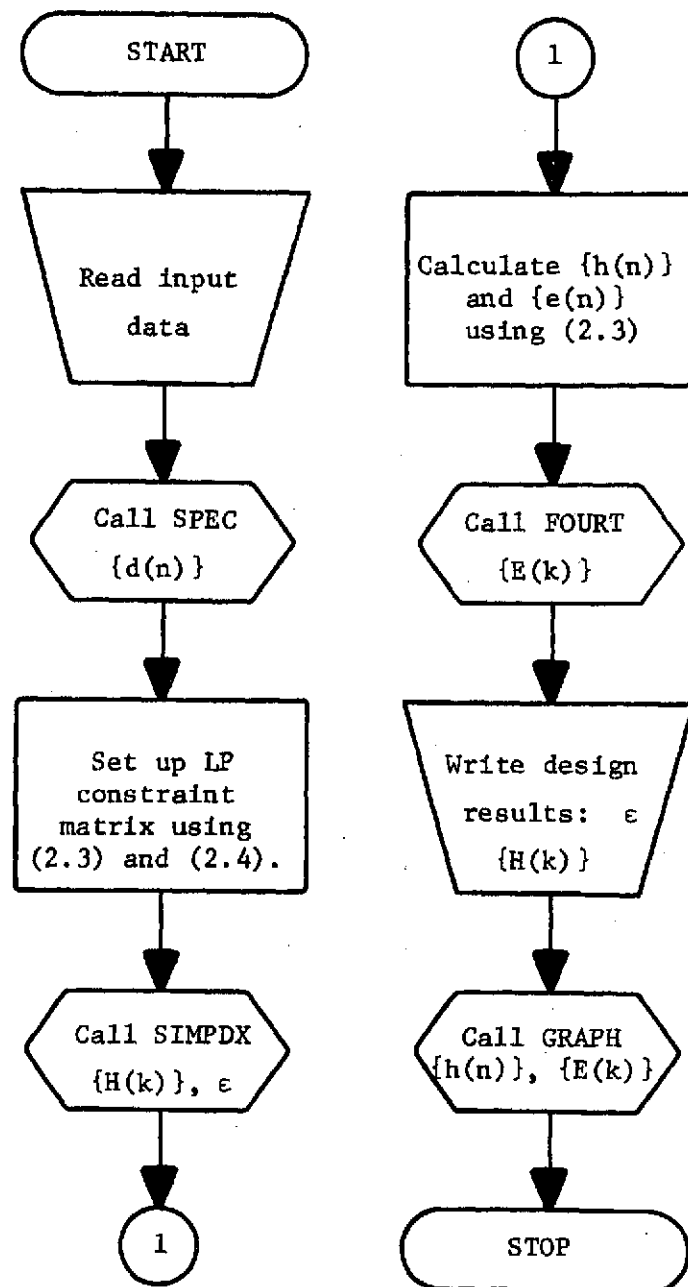


Fig. B-1. Minimax Pulse Shaping
Digital Filter Design Program.

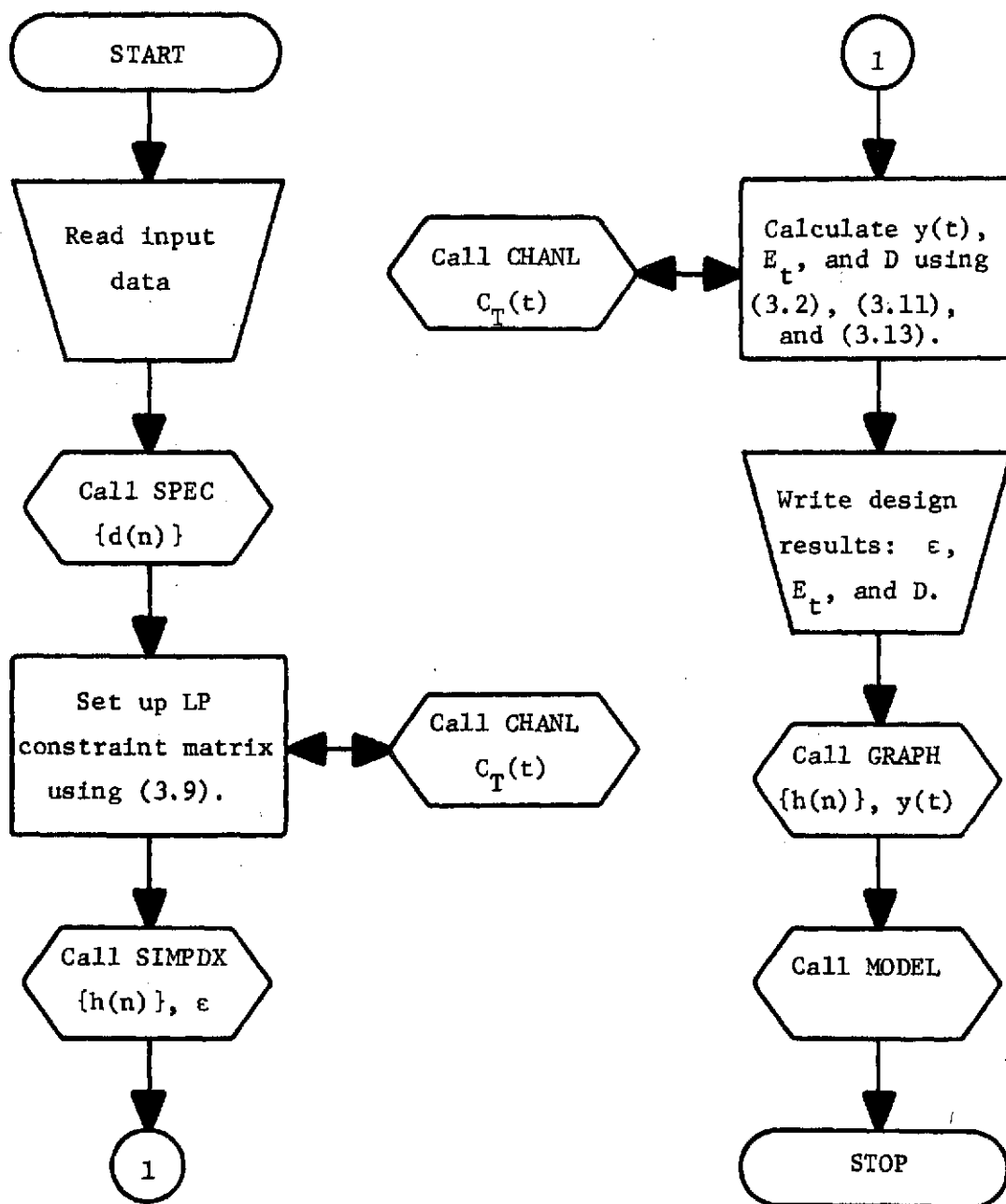


Fig. B-2. PSRCT, Minimax Transversal Equalizer Design Program.

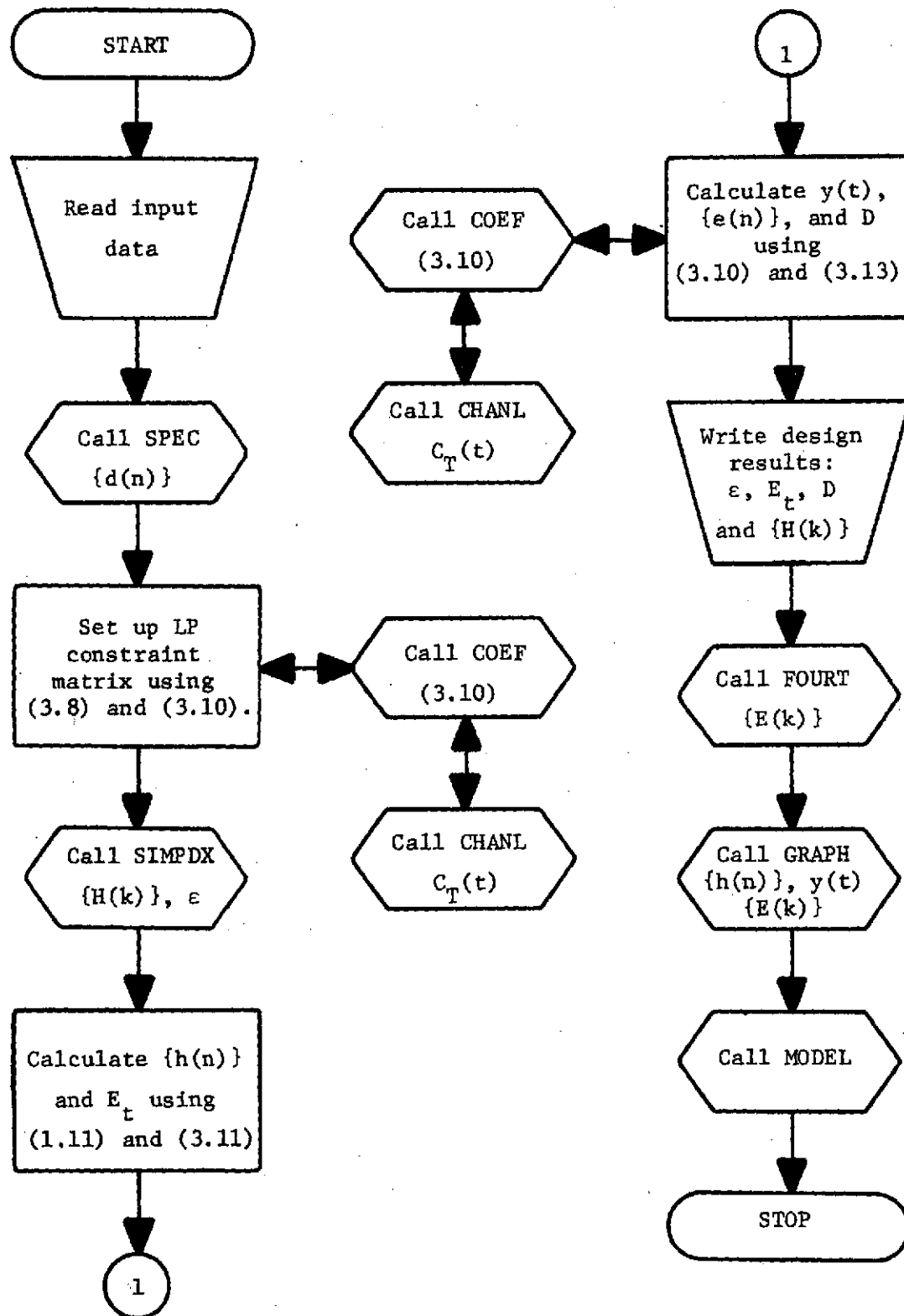


Fig. B-3. PSRCF, Minimax Frequency-Sampling Equalizer Design Program.

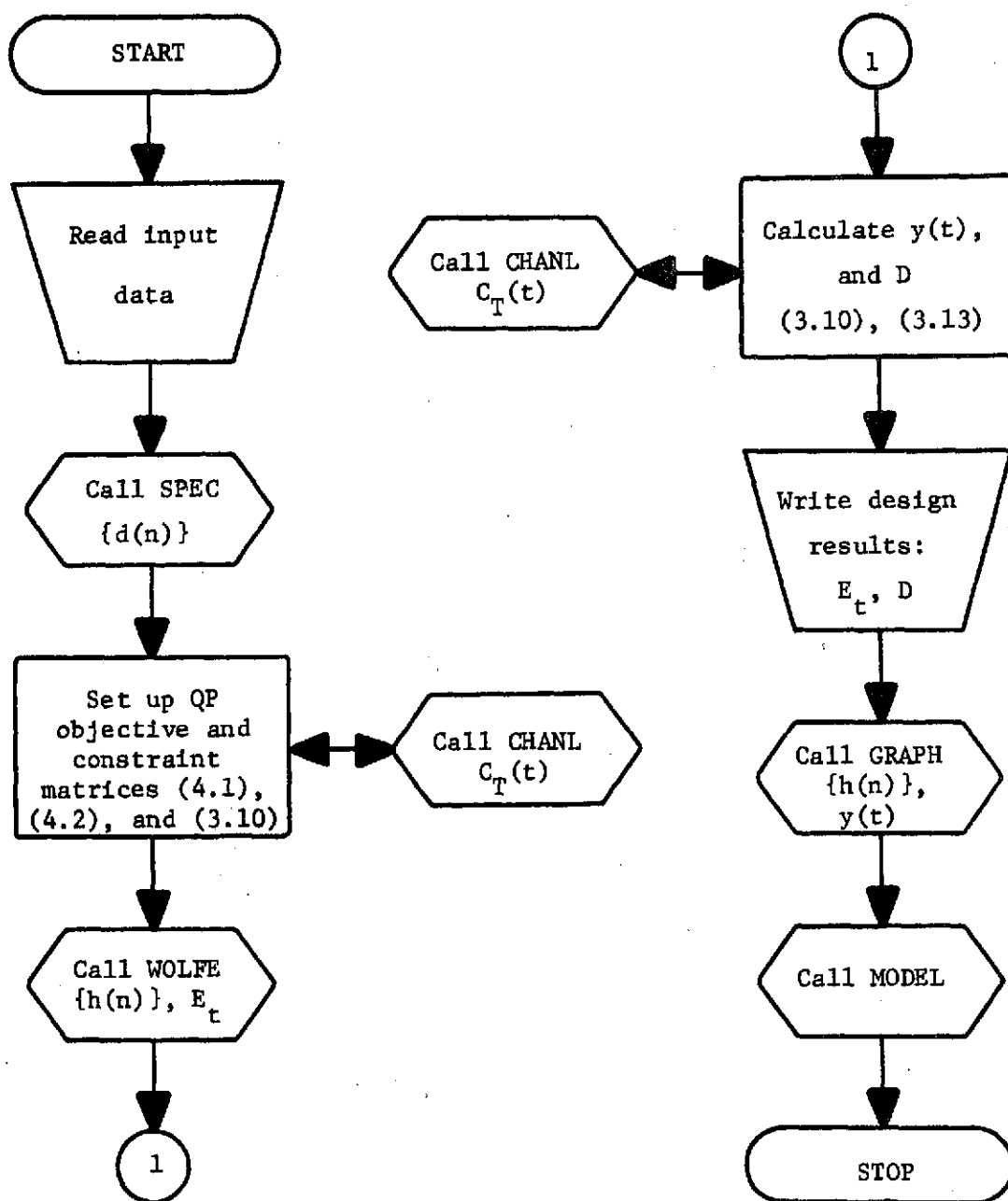


Fig. B-4. EMRCT, Energy-Minimization Transversal Equalizer Design Program.

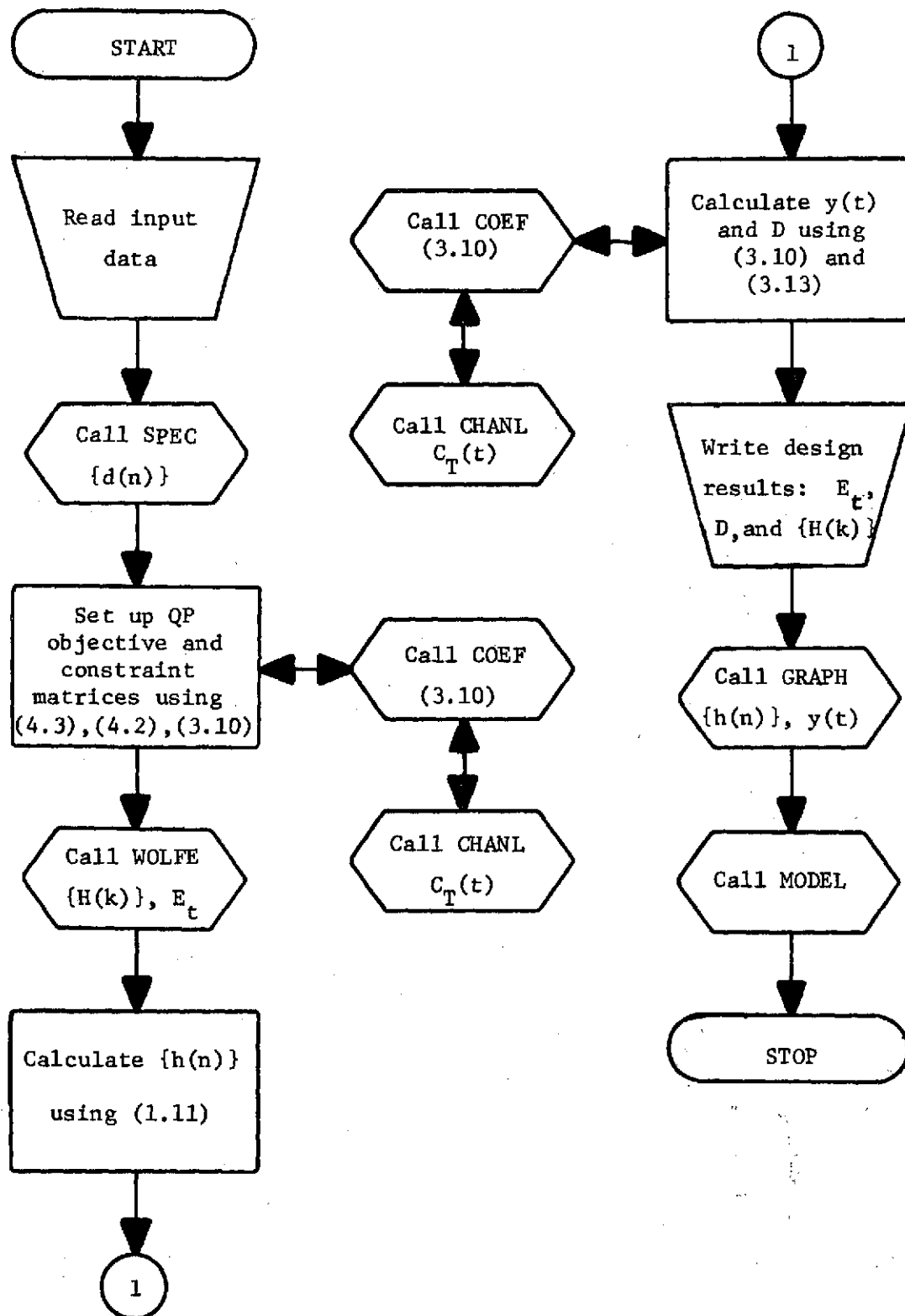


Fig. B-5. EMRCF, Energy-Minimization Frequency-Sampling Equalizer Design Program.

TABLE B.1

INPUT DATA FOR DESIGN PROGRAMS

	PSIC	PSRCF	PSRCT	EMRCF	EMRCT
Name of desired pulse	X	X	X	X	X
N, number of samples	X	X	X	X	X
B, samples per baud interval	X	X	X	X	X
R, number of resonators	X	X		X	
{S(i)}, which resonator	X	X		X	
T_b , baud time interval		X	X	X	X
Name of channel model		X	X	X	X
T_d , delay of channel		X	X	X	X
ϵ , allowed error				X	X

B.2 AUXILIARY SUBPROGRAMS

Several auxiliary subprograms are called by the main design programs to do specific functions. A brief description of the operation of these subprograms is given in this section.

Subroutine SPEC produces samples of the desired received waveform $y(t)$ using as input the name of the waveform, the number of samples, the number of samples per baud interval, and the delay of the channel. For the Minimax designs SPEC returns N equally-spaced samples of the desired waveform. For the Energy-Minimization designs SPEC returns time values corresponding to the zero crossings and/or baud times of the waveform as well as samples at these times.

Subroutine COEF calculates the coefficients of $X(k)$ and $Y(k)$ in equation (3.10). It calls CHANL to obtain the impulse response of the channel model.

Subroutine CHANL uses as input the name of the channel model to be used and a time value t . It returns the value of the channel impulse response at t , $c_T(t)$. For the channel models derived from measurements, CHANL calls the Spline interpolation routines SPLN1 and SPLN2 to produce a continuous, smooth curve through the measured points in the channel's impulse response.

Subroutine GRAPH produces printer-plots of a waveform. It uses as input a set of equally-spaced samples of the waveform.

Subroutine MODEL simulates the transmission of a 15 bit PN sequence through the equalized channel. Bipolar unit pulses are applied to the equalizer input at the rate of $1/T_b$. The equalizer output and the channel output are recorded using GRAPH.

LIST OF REFERENCES

1. H. Nyquist, "Certain topics in telegraph transmission theory," Trans. AIEE, vol. 47, pp. 617-644, April 1928.
2. J. M. Wozencraft and I. M. Jacobs, Principles of Communication Engineering, New York: John Wiley & Sons, 1967, Chapter 4.
3. R. W. Lucky, J. Salz, and E. J. Weldon, Jr., Principles of Data Communication, New York: McGraw-Hill, 1968, Chapters 3 and 5.
4. Ibid., Chapter 4.
5. C. M. Rader and B. Gold, "Digital filter design techniques in the frequency domain," Proc. IEEE, vol. 55, pp. 149-171, February 1967.
6. R. C. Houts and D. W. Burlage, "The use of linear programming techniques to design optimal digital filters for pulse shaping and channel equalization," University of Alabama Bureau of Engineering Research Technical Report No. 142-102, April 1972.
7. J. C. Hancock, H. Schwarzlander, and R. E. Totty, "Optimization of pulse transmission," IEEE Proceedings, vol. 50, p. 2136, October 1962.
8. F. C. Schweppe, "Optimization of signals," Lincoln Laboratory Massachusetts Institute of Technology Technical Report No. AF 19(628)-500, January 1964.
9. D. L. Snyder and G. J. Blaine, "Signal design for channels with known time-dispersion," National Telecommunications Conference, vol. CHO 601-5-NTC, pp. 15A-1 to 15A-4, December 1972.
10. L. R. Rabiner, "Techniques for designing finite-duration impulse-response digital filters," IEEE Trans. Communication Technology, vol. COM-19, pp. 188-195, April 1971.
11. L. R. Rabiner and R. W. Schafer, "Recursive and nonrecursive realizations of digital filters designed by frequency sampling techniques," IEEE Trans. Audio and Electroacoustics, vol. AU-19, pp. 200-207, September 1971.

12. L. R. Rabiner, "The design of finite impulse response digital filters using linear programming techniques," Bell System Technical Journal, vol. 51, pp. 1117-1198, July-August 1972.
13. L. R. Rabiner, "Approximate design relationships for low-pass FIR digital filters," IEEE Trans. Audio and Electroacoustics, vol. AU-21, pp. 456-460, October 1973.
14. J. H. McClellan, T. W. Parks, and L. R. Rabiner, "A computer program for designing optimum FIR linear phase digital filters," IEEE Trans. Audio and Electroacoustics, vol. AU-21, pp. 506-526, December 1973.
15. R. K. Cavin, C. H. Ray, and V. T. Rhyne, "The design of optimal convolutional filters via linear programming," IEEE Trans. Geoscience Electronics, vol. GE-7, pp. 142-145, July 1969.
16. H. D. Helms, "Digital filters with equiripple or minimax responses," IEEE Trans. Audio and Electroacoustics, vol. AU-19, pp. 87-93, March 1971.
17. D. W. Burlage and R. C. Houts, "The use of linear programming to design digital filters from impulse-response specifications," Proceedings of the 10th Annual IEEE Region 3 Convention, no. 72 CHO 591-8, April 1972.
18. D. W. Burlage and R. C. Houts, "Applications of linear programming to the time-domain design of digital-filter equalizers," IEEE Trans. Communications, vol. COM-21, pp. 1417-1422, December 1973.
19. R. J. Westcott, "An experimental adaptively equalized modem for data transmission over the switched telephone network," Conference on Digital Processing of Signals in Communications, Loughborough, Leics., England, pp. 195-212, April 1972.
20. Large Scale Systems Math-Pack Programmers Reference, Sperry Rand Corporation, 1967, pp. 2-68 to 2-74.
21. R. S. Simpson and R. C. Houts, Fundamentals of Analog and Digital Communication Systems, Boston: Allyn and Bacon, 1971, pp. 104-110.
22. S. I. Gass, Linear Programming, New York: McGraw-Hill, 1958, pp. 1-189.
23. H. P. Künzi and W. Krelle, Nonlinear Programming, Waltham, Massachusetts: Blaisdell Publishing Company, 1966, pp. 71-225.
24. B. Gold and C. M. Rader, Digital Processing of Signals, New York: McGraw-Hill, 1969, pp. 159-202.

25. G. Diderrich, SIMPDX/SIMPLX Linear Programming Subroutines, Madison, Wisconsin: The University of Wisconsin Computing Center, 1970.
26. W. I. Zangwill, Nonlinear Programming: A Unified Approach, Englewood Cliffs, New Jersey: Prentice-Hall, 1969, pp. 158-212.
27. P. Wolfe, "The simplex method for quadratic programming," Econometrica, vol. 27, pp. 382-398, July 1959.
28. N. Brenner, Cooley-Tukey Fast Fourier Transform in USACI Basic FORTRAN, MIT Lincoln Laboratory, 1968.
29. G. L. Vaughn, "FORTRAN programs for design of FIR digital filters for pulse shaping and channel equalization using time-domain optimization," Technical Note #1 for Technical Report No. 167-102, May 1974.

COMMUNICATION SYSTEMS GROUP

RECENT REPORTS

A Digital Technique to Compensate for Time-Base Error in Magnetic Tape Recording, R. S. Simpson, R. C. Houts and D. W. Burlage, August, 1968.

A Study of Major Coding Techniques for Digital Communication, R. S. Simpson and J. B. Cain, January, 1969.

Study of Correlation Receiver Performances in the Presence of Impulse Noise, R. C. Houts and J. D. Moore, February, 1971.

Computer-Aided Design of Digital Filters, R. C. Houts and D. W. Burlage, March, 1971.

Characterization of Impulse Noise and Analysis of Its Effects upon Correlation Receivers, R. C. Houts and J. D. Moore, October, 1971.

The Use of Linear Programming Techniques to Design Optimal Digital Filters for Pulse Shaping and Channel Equalization, R. C. Houts and D. W. Burlage, April, 1972.

A Comparative Analysis of Digital Baseband Signals, R. C. Houts and T. A. Green, June, 1972.

A Fast-Initializing Digital Equalizer With On-Line Tracking for Data Communication, R. C. Houts and W. J. Barksdale, May, 1974.